Biomicrofluidics REVIEW scitation.org/journal/bmf

From cell spheroids to vascularized cancer organoids: Microfluidic tumor-on-a-chip models for preclinical drug evaluations

Cite as: Biomicrofluidics **15**, 061503 (2021); doi: 10.1063/5.0062697
Submitted: 7 July 2021 · Accepted: 16 October 2021 ·
Published Online: 9 November 2021

Yue Wu,[1] Yuyuan Zhou,[1] Xiaochen Qin,[1] and Yaling Liu[1,2,a)]

AFFILIATIONS

[1]Department of Bioengineering, Lehigh University, Bethlehem, Pennsylvania 18015, USA
[2]Department of Mechanical Engineering and Mechanics, Lehigh University, Bethlehem, Pennsylvania 18015, USA

[a)]**Author to whom correspondence should be addressed:** yal310@lehigh.edu

ABSTRACT

Chemotherapy is one of the most effective cancer treatments. Starting from the discovery of new molecular entities, it usually takes about 10 years and 2 billion U.S. dollars to bring an effective anti-cancer drug from the benchtop to patients. Due to the physiological differences between animal models and humans, more than 90% of drug candidates failed in phase I clinical trials. Thus, a more efficient drug screening system to identify feasible compounds and pre-exclude less promising drug candidates is strongly desired. For their capability to accurately construct *in vitro* tumor models derived from human cells to reproduce pathological and physiological processes, microfluidic tumor chips are reliable platforms for preclinical drug screening, personalized medicine, and fundamental oncology research. This review summarizes the recent progress of the microfluidic tumor chip and highlights tumor vascularization strategies. In addition, promising imaging modalities for enhancing data acquisition and machine learning-based image analysis methods to accurately quantify the dynamics of tumor spheroids are introduced. It is believed that the microfluidic tumor chip will serve as a high-throughput, biomimetic, and multi-sensor integrated system for efficient preclinical drug evaluation in the future.

INTRODUCTION

Today, cancer has become one of the most atrocious threats to human health. It is estimated that by 2021, there will be nearly 2×10^6 new cancer cases and more than 600 000 cancer deaths in the United States.[1] Besides radiotherapy and surgical resection, chemotherapy is the most common and reliable anti-cancer treatment.[2] Although cancer pharmacological treatment has made great progress in the past decade, it is still challenging to effectively discover and develop new anti-cancer drugs.[3] In general, it takes over 10 years to bring an effective drug from research to clinic.[4] In the drug development process, drug candidate screening is one of the most important but time-consuming stages. Herein, an appropriate preclinical tumor model can effectively eliminate unqualified drug candidates and improve screening efficiency. Traditionally, animal models have played a vital role in oncology research and drug testing. However, these methods are limited by the long experimental period, excessive number of animals consumed, high maintenance cost of the facility, and social ethics. In addition, the tumor characteristics from clinical patients and animal models vary greatly. Therefore, there is still a huge disparity between the efficacy of drug candidates in animal models and the final results of clinical patients, which often leads to misjudgments in drug test, increases in R&D costs, and extensions of the development cycle.[5]

Since the new century, cellular-level drug screening technology has gradually matured. Tumor models derived from human cells are used to quantitatively characterize cell viability, morphogenesis, proliferation, and gene expression under the action of different drug candidates.[6] For a long time, the two-dimensional (2D) monolayer cancer model has been a mainstream *in vitro* oncology model for early preclinical drug screening and testing. However, 2D adherent growth is not the actual way of cell growth in the human body. Lack of cell-to-cell and cell-to-extracellular matrix (ECM) interactions lead to altered cell behaviors, such as gene expression, differentiation, and cell metabolism.[7] Significantly, the physiological correlation between the *in vitro* model used for drug evaluation and the real tumor from patients is very critical. The more realistic

the *in vitro* model, the more reliable the preclinical drug screening.[8] Currently, most of the anti-cancer drug candidates screened by 2D models failed to pass clinical trials in the later stages.[9]

Nowadays, three-dimensional (3D) cellular models for drug testing have been widely studied and are attracting more and more attention.[10] Compared to the conventional 2D monolayer cell culture model, 3D cell culture allows cells to grow in all directions and recapitulate more *in vivo* behaviors and functions, such as self-organization, proliferation, and protein expression.[11] Among them, 3D multicellular tumor spheroid is one of the most used models for preclinical anti-cancer drug screening (Fig. 1). Based on microfluidic technology, tumor spheroids can be manufactured through standardized on-chip production, thereby reducing the individual differences between models, and improving reproducibility and consistency. In addition, the tumor microenvironment (TME) can also be restored in the on-chip microphysiological system to accurately reproduce the tumor–microenvironment interaction.[12] Eventually, the microfluidic tumor chip technology is believed to play an important role in advancing fundamental cancer biology research, high-throughput preclinical drug screening, and precise personalized medicine.[13]

In view of the vigorous development of the field of microfluidic tumor chips, many review articles have been published.[14] Some of them introduced the biological background of tumor spheroid in detail,[15,16] some were devoted to the advanced fabrication technology,[17,18] and some were focused on constructing the complex tumor microenvironment.[19,20] This review will serve as a bridge to link the preceding accomplishment and the following advancement. Besides summarizing the latest representative achievements of microfluidic tumor chips, we will make a comprehensive review of microfluidic tumor chips in the order from homotypic tumor spheroid fabrication to vascularization-based tumor microenvironment construction. Meanwhile, as the source technology of microfluidic tumor chips, organ on a chip technology will also be briefly introduced. Finally, we will present some classic cases of novel imaging methods for data acquisition and machine learning-based image analysis to accurately quantify tumor spheroid dynamics. We hope that this review will help researchers get the basic engineering concepts for constructing microfluidic tumor models and encourage new ideas in the future.

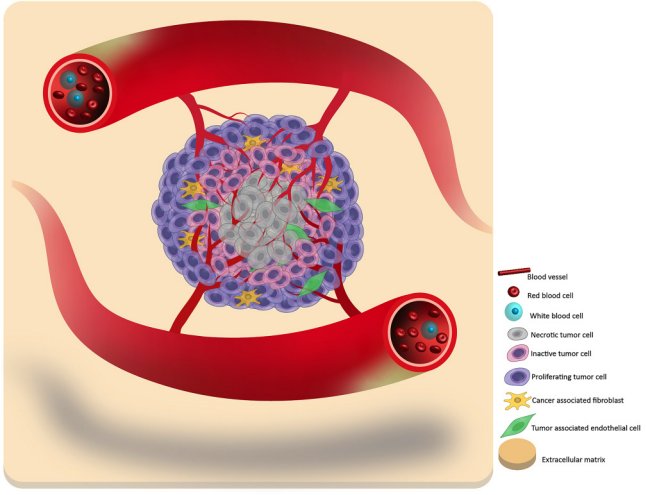

FIG. 1. A schematic of the primary tumor structure and composition. In general, a tumor can be considered to contain three layers: the necrotic core, the inactive quiescent middle layer, and the proliferative outer layer. By hijacking the surrounding blood vessels, the tumor cells can obtain oxygen and nutrients to promote their growth. In addition, some tumors can also incorporate the surrounding tissue into a part of itself, such as cancer-associated fibroblasts and tumor-associated endothelial cells, which increases the tumor heterogeneity and complexity.

CONVENTIONAL TUMOR CELL SPHEROID MODEL CONSTRUCTION TECHNIQUES

Cell self-assembly has always been the natural law guiding the formation of all living organisms, whether *in vitro* or *in vivo*.[21] When cancer cells cannot adhere to the substrate in the *in vitro* environment, they will spontaneously aggregate and secrete extracellular matrix to wrap themselves into multicellular tumor spheroids.[22] In early studies, the manufacture of tumor spheroids was often out of touch with the subsequent drug screening process. For instance, agitation-based approach was one of the early methods for generating tumor spheroids.[23] However, most of these methods lack guarantees on the size and viability of mass-produced tumor spheroids. When the tumor spheroids were collected for further experiments, these by-effects would cause a certain degree of interference to the final experimental results.

In the past ten years, microfluidic tumor chip technologies have emerged rapidly. The basic idea of microfluidic tumor spheroids manufacturing is to build micro-reactors to create non-attachable space, leading to cell self-assembly.[24–31] Initially, the hanging drop method is one of the most classic and well-established tumor spheroid fabrication methods.[32,33] The balance between surface tension and gravity keeps the droplets converging on the surface of the substrate without falling. Here, the droplets function as the micro-reactors and the liquid–air interface functions as the non-attachable substrate to prevent cell adhesion. The suspended cells will aggregate into spheroids at the bottom of the droplet under gravity, and the spheroid size will be dependent on the droplet dimension and initial cell concentration. Tung *et al.* reported a hanging drop based 3D tumor spheroid culture platform in 2011 [Fig. 2(a)].[34] Developed tumor spheroids were able to form in one day, and diverse preclinical drug screening could be executed in each hanging droplet respectively.

Nowadays, to break through the limitation of tedious manual operation, the hanging drop technology continues to develop in the direction of automation and high-throughput. Recently, Popova *et al.* reported a "droplet-microarray platform" for one-stop tumor spheroid formation and drug screening [Fig. 2(b)].[35] They used hydrophilic–superhydrophobic patterning to create a hanging droplet array on hydroxyethyl-methacrylate (HEMA)–ethylene dimethacrylate (EDMA) slides. Due to the great difference in water affinity between the hydrophilic and superhydrophobic parts of the surface, an array of separated homogeneous droplets could spontaneously form on the device surface. Also, Michael *et al.* reported a paper-based hanging drop chip for tumor spheroid fabrication [Fig. 2(c)].[36] Zhao *et al.*

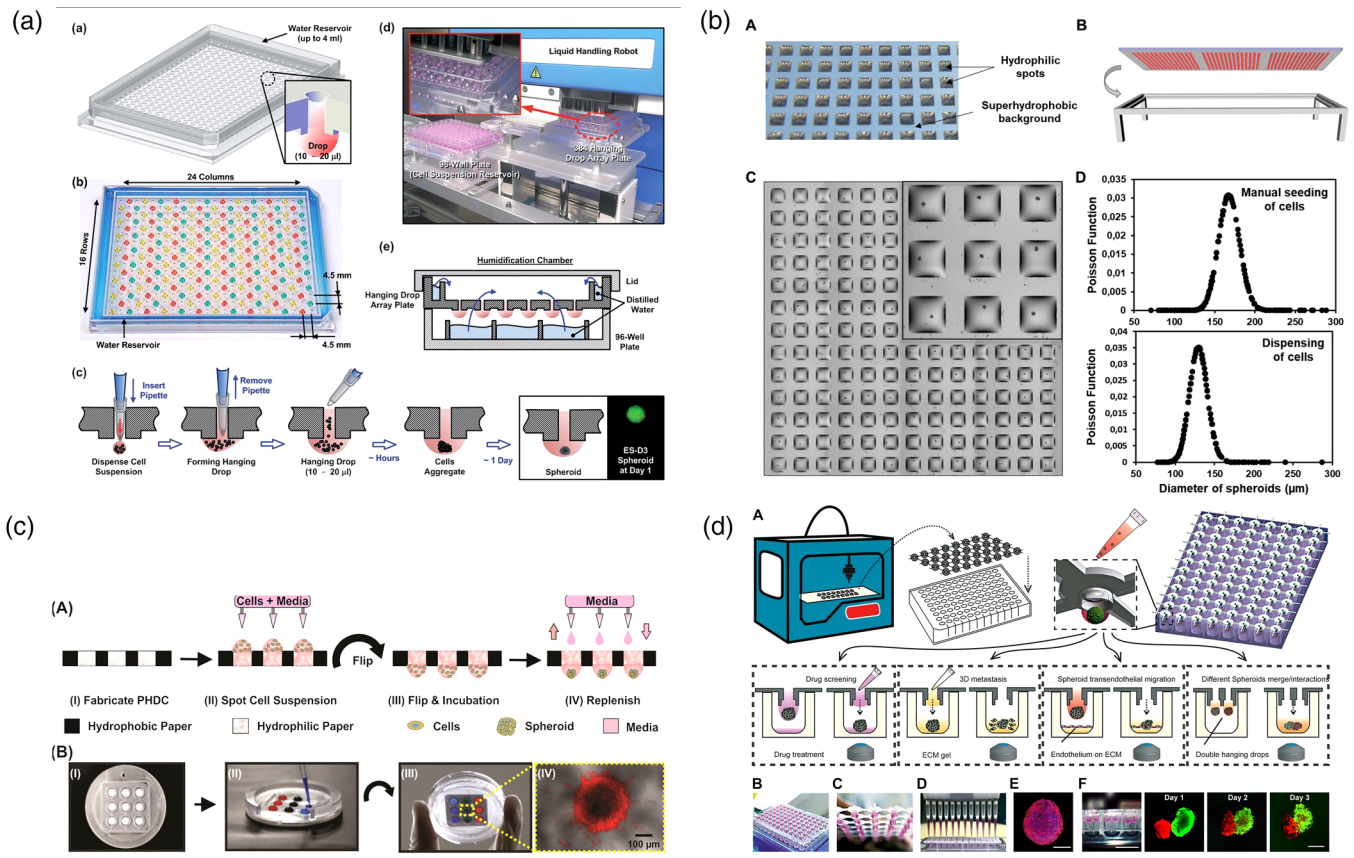

FIG. 2. Conventional "hanging drop method" for producing tumor spheroids for drug screening. (a) A 384-well format hanging drop culture plate that allows both tumor spheroid formation and subsequent drug testing.[34] Reprinted with permission from Tung *et al.*, Analyst **136**, 473 (2011). Copyright 2011 Royal Society of Chemistry. (b) A droplet-microarray platform based on hydrophilic–superhydrophobic patterning for the formation of single tumor spheroids array.[35] Reprinted with permission from Popova *et al.*, Small **15**, e1901299 (2019). Copyright 2019 WILEY-VCH Verlag GmbH & Co. KGaA, Weinheim. (c) A paper-based hanging drop chip for large scale tumor spheroids formation at low cost.[36] Reprinted with permission from Michael *et al.*, ACS Appl. Mater. Interfaces **10**, 33839 (2018). Copyright 2018 American Chemical Society. (d) A 3D-printed hanging drop dripper for automated tumor spheroids generation, metastatic migration study, and drug screening.[37] Reprinted with permission from Zhao *et al.*, Sci. Rep. **9**, 19717 (2019). Copyright 2019 Springer Nature.

announced a 3D-printed hanging drop dripper product. The printed artifact is simple and practical and can be directly mounted on the conventional 96/384-well plate [Fig. 2(d)].[37] Compared to the traditional hanging drop methods, these innovative works simplify device fabrication, prove the possibility of further reducing costs, and pave the way for potential commercialization in the future. However, the hanging drop technology is usually limited by its inherent flaws. Due to the fragile structure of the liquid droplets, it was still difficult to change the culture medium for long-term tumor spheroid culture, which leads to fast nutrient depletion and waste accumulation. Moreover, all the spheroids were cultured in a purely static environment, while some mechanical stimulations, such as interstitial flow, have been demonstrated to better support tumor growth.[38] Although not perfect, the hanging drop approaches are still considered the pioneering work to link the tumor spheroids generation and the following drug testing.

MICROFLUIDIC TUMOR-ON-A-CHIP

Microfluidic fabrication of homotypic tumor spheroid-on-a-chip

Since the new century, the maturity of microelectromechanical systems (MEMS) technology greatly boosts the development of the microfluidic tumor chip.[39,40] Photolithography, vapor deposition, and other micro-processing techniques have enabled the preparation of some complex microstructures, which are necessary for precise manipulation of microscale chemical reagents and perfusion. Moreover, more and more electronic biochemical sensors are also coupled into the microfluidic tumor chip system.[41] Consequently, real-time *in situ* monitoring of tumor response allows drug screening with much higher temporal and spatial resolution. It can be said that now the microfluidic tumor chip technology is right in the golden ages.

The most common application of a microfluidic tumor chip is serving as a one-stop platform, seamlessly connecting tumor spheroid model construction and preclinical drug screening for oncology research.[45–50] In such systems, single tumor spheroids can be generated and maintained at fixed locations for drug screening and follow-up characterization. The basic microfluidic tumor chips can be classified into the following two categories: microwell[42,51–60] [Fig. 3(a)] and U-shaped microanchor[44,61–66] [Fig. 3(b)]. These two designs are similar in function but different in shape. In general, these chips are composed of the main fluid channel and the structure array.[67] After being loaded into the main fluid channel, suspended tumor cells are captured by each microstructure. The trapped cells have no place to attach but to self-assemble into the tumor spheroids. After tumor spheroid formation, the function of the main channel will turn to medium exchange and drug administration [Fig. 3(a)].[42] Since the established tumor spheroids are firmly stuck by the microstructures, dynamic fluid flow can continue to be applied in the main channel without harassing the spheroids or carrying them away. This perfusion function facilitates the long-term tumor spheroids culture, which is usually limited in the hanging drop methods. Some studies also reported that appropriate mechanical perturbation of the flow can promote tumor growth since it mimics the interstitial flow in *in vivo* tumor tissue to a certain extent.[68]

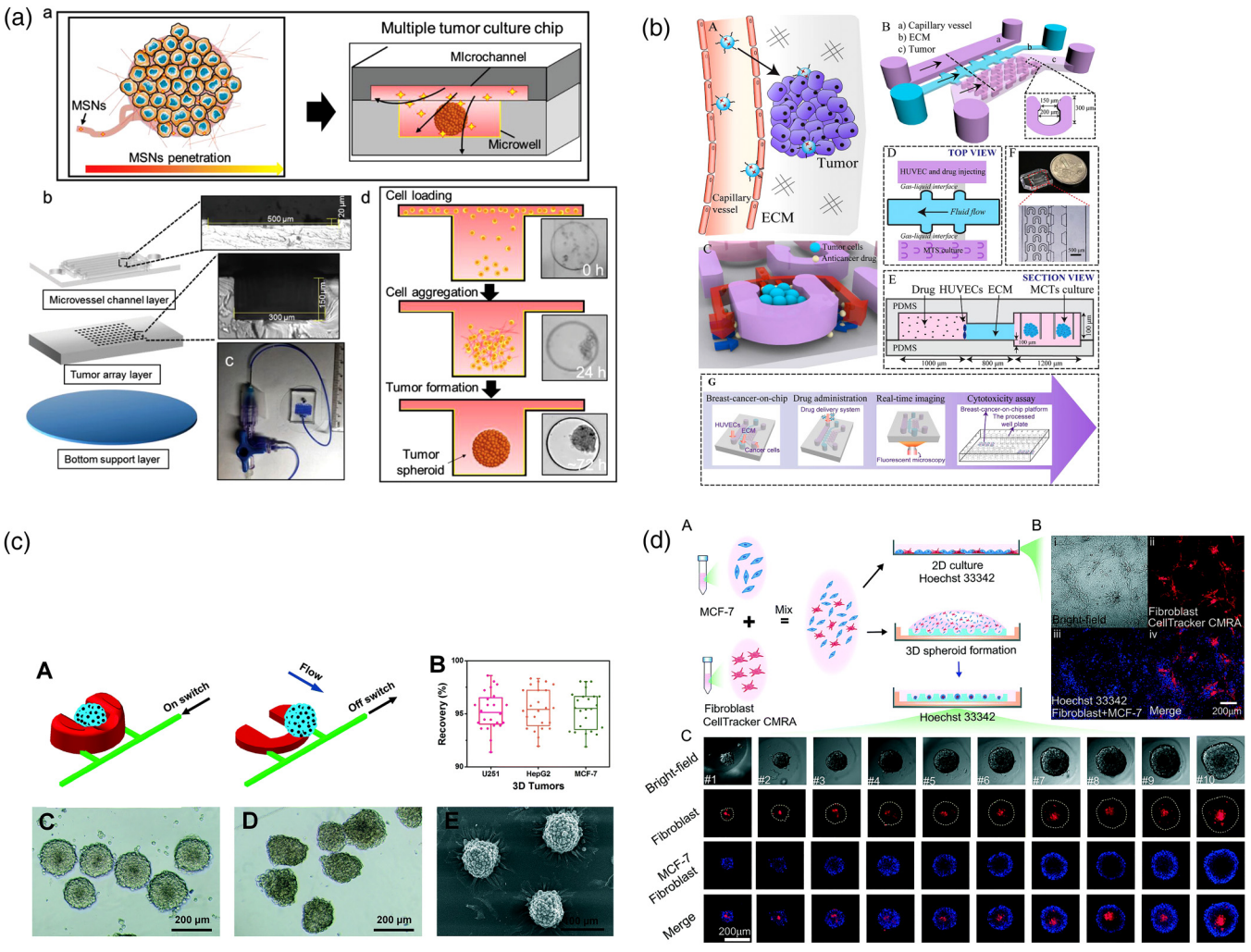

FIG. 3. Classic "microfluidic tumor chip" designs. (a) Microwell-based multiple tumor spheroids culture chip (MTC-chip) cultured tumor under various flow conditions.[42] Reprinted with permission from Zhuang *et al.*, Adv. Sci. **6**, 1901462 (2019). Copyright 2019 WILEY-VCH Verlag GmbH & Co. KGaA, Weinheim. (b) A U-shaped array based 3D breast-cancer-on-a-chip for the evaluation of nanoparticle-based drug delivery systems.[43] Reprinted with permission from Chen *et al.*, Anal. Chim. Acta **1036**, 97 (2018). Copyright 2018 Elsevier B.V. (c) Pneumatically actuated U-shaped arrays for one-step cell localization, spheroids self-assembly, and real-time analysis.[44] Reprinted with permission from Liu *et al.*, Lab Chip **15**, 1195 (2015). Copyright 2015 The Royal Society of Chemistry. (d) Liquid dome-assisted formation of gradient-sized spheroids on an agarose chip.[29] Reprinted from Fang *et al.*, Lab Chip **19**, 4093 (2019). Copyright 2019 The Royal Society of Chemistry.

With the advancement of fabrication technology, the structure of the microfluidic tumor chips becomes more and more dynamic and flexible. In these specific cases, the conventional sealed microfluidic tumor chips described above would be inconvenient for retrieving the tumor spheroids for downstream analysis. To solve this problem, Liu *et al.* integrated a flexible pneumatic microanchor array design with the conventional U-shaped tumor chip [Fig. 3(c)].[44,66] When the pneumatic switch was turned on, the inflatable anchor would stand upright to capture the suspended tumor cells. After nanomedicine treatment, the tumor spheroids from the chip could be selectively carried out by turning off the pneumatic microstructures. The recovery feature builds up a practical bridge between tumor-on-a-chip modeling and off-chip pathological characterization. In addition to pursuing a complex microfluidic tumor chip design, some groups, on the contrary, further simplify the chip manufacturing process and make it easier to operate. For example, Fang *et al.* reported an agar microfluidic tumor chip that can produce a tumor spheroid with only 250 μl cell suspension [Fig. 3(d)].[29] Benefiting from a 3D-printed mold, an agar chip can be easily generated through the molding method, which is more advantageous for routine laboratories and easy to popularize.

High-throughput fabrication of tumor spheroid via the microfluidic droplet technique

Besides solid microstructures, liquid microstructures can also be engaged in tumor spheroid modeling. Microfluidic droplet-based techniques stand out for their high-throughput and uniformity.[70,73–76] In the channel of the microfluidic chip, two continuous fluids that are immiscible with each other will generate a stable and ordered non-continuous flow at the interface, which is the so-called microdroplets. By adjusting the chip design and the flow rate of the two-phase liquid, the size, shape, and frequency of the microdroplets can be precisely regulated.[77] In particular, the water-in-oil (W/O) emulsion is the most used system for tumor spheroid preparation. A suspended cell-laden medium is wrapped into microdroplets and immersed in a continuous oil phase. These microdroplets can function as the bioreactors leading to the tumor spheroid formation in days. In some way, microdroplet-based tumor spheroid construction methods are like a "fully automatic version" of the conventional "hanging drop" method. The difference lies in that the cell-laden droplets are immersed in the culture medium instead of sticking to the plate. Kwak *et al.* reported a uniform-sized 3D tumor spheroid fabrication system in 2018 [Fig. 4(a)].[69] Cell-loaded microdroplets could be generated at a rate of 1000 droplets/min. After 24-hour incubation, mature tumor spheroids were released from the oil capsule and recollected for downstream anti-cancer drug testing. Therefore, the microdroplet is considered one of the most efficient techniques to fabricate tumor spheroids. However, the oil capsule shells limit the exchange of the nutrient medium. The mature tumor spheroids need to be timely released from the microdroplets after one day; otherwise, the nutrients in the droplets will be exhausted. Without the microfluidic chamber's restriction, the tumor spheroids that were mass-produced in a short time can be recollected, transferred, and applied to a variety of tests, such as photothermal therapy (PTT) [Fig. 4(b)].[70]

Moreover, if the water phase is replaced with the pre-gel solution, the cell-laden microdroplets can be cured into 3D cell-laden hydrogel beads later [Fig. 4(c)].[71] It has been reported that the cured hydrogel can serve as a scaffold, which facilitates the tumor spheroid formation.[72,78,79] After being washed out from the oil phase, the tumor structures can still be maintained stably in hydrogel beads until spheroid maturation. Sabhachandani *et al.* improved the microfluidic droplet technique with an "anchor array" design [Fig. 4(d)].[72] In this system, cells are loaded in alginate beads. Once the alginate gets solidified, the oil phase can be washed away with a medium without disrupting the cell spheroids. The tumor spheroids in alginate beads can be trapped on the chip for long-term culture until spheroid maturation for dynamic drug screening.[80] This technique inherits the advantages of rapid fabrication of the microdroplet system and the conventional microwell-based tumor chip, while being more flexible, practical, and straightforward for drug testing.

Device-less manufacturing of tumor spheroids

Recently, more innovative materials and interdisciplinary elements are introduced into the microfluidic "tumor chip" design. Based on the concept of microfluidics, some device-free and device-less technologies have been developed accordingly for tumor spheroid fabrication.[81] For example, Samara *et al.* tried to substitute traditional polydimethylsiloxane (PDMS) material with paper to fabricate a "tumor chip" for drug screening, which is claimed to be a more cost-efficient experimental procedure.[82] Also, Shi *et al.* reported a device-free way to generate tumor spheroids for drug screening.[83] By rolling up detached cell sheets, a large quantity of tumor spheroids can be formed with controllable size and high uniformity. As for device-less approaches, magnetic levitation is one of the latest emerging trends for scaffold-free tumor spheroid model construction.[84–88] Activated by an external magnetic field, cells labeled with magnetic nanoparticle are gathered into cell clusters. Ho *et al.* can even directly magnetically pattern HeLa tumor spheroids into the desired topography.[85] Similarly, acoustics is another popular element that frequently shows up in tumor spheroid-related studies.[89–92] In acoustic scenarios, cells are compressed and reallocated together by the mechanical sound waves propagating in the medium. Rather than passively waiting cells to migrate together, these proactive manipulations can assemble cells in a rapid way, which greatly shortens the bio-fabrication time. These device-less methods rely more on external physics systems rather than sophisticated microfluidic chamber designs. However, these interdisciplinary technologies still need to be optimized. For example, magnetic bead-labeled on cells are usually hard to be removed later. It is difficult to guarantee that these remaining beads will not have any effect on the subsequent growth of the cells. In general, there is still a long way to go to integrate these new elements into the desired "all-in-one" tumor chip system (tumor formation, drug screening, and post-analysis).[93,94]

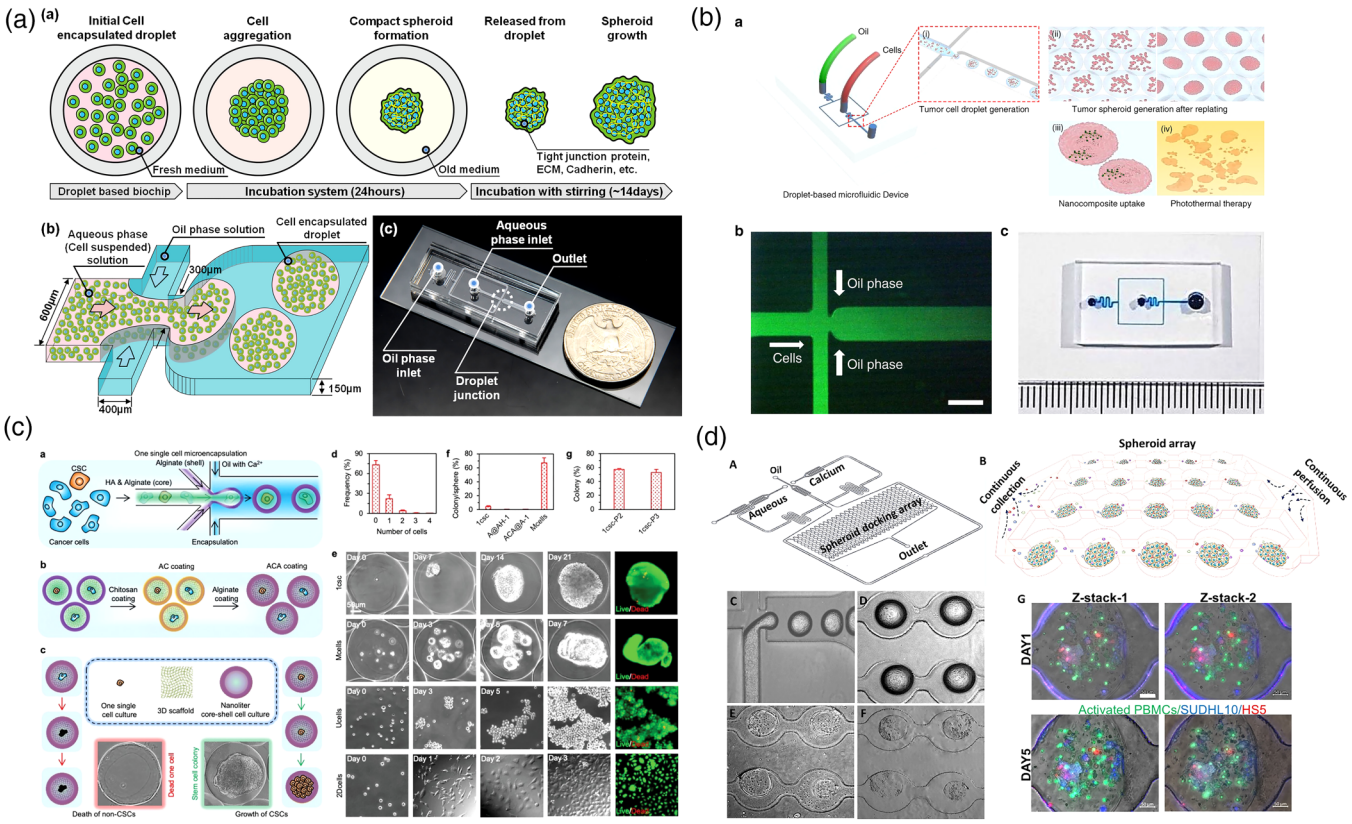

FIG. 4. Microdroplet technique for high-throughput tumor spheroid generation. (a) A droplet-based microfluidic system that generates cancer cells containing microdroplets at high yield (1000 droplets/min).[69] Reprinted with permission from Kwak *et al.*, J. Controlled Release **275**, 201 (2018). Copyright 2018 Elsevier B.V. (b) Size-tunable brain tumor spheroids generated by microfluidic droplets are applied for photothermal therapy (PTT) testing.[70] Reprinted with permission from Lee *et al.*, Microsyst. Nanoeng. **6**, 52 (2020). Copyright 2020 Springer Nature. (c) A droplet-based microfluidic device for constructing tumor spheroids from single cancer cells.[71] Reprinted with permission from Wang *et al.*, Adv. Sci. **7**, 2000259 (2020). Copyright 2020 WILEY-VCH Verlag GmbH & Co. KGaA, Weinheim. (d) An integrated droplet-based microfluidic platform for dynamic analysis of cellular interaction, proliferation, and therapeutic efficacy via spatiotemporal profiling on chip.[72] Reprinted with permission from Sabhachandani *et al.*, J. Controlled Release **295**, 21 (2019). Copyright 2018 Elsevier B.V.

MODELING TUMOR-VASCULATURE INTERACTIONS IN MICROFLUIDIC PHYSIOLOGICAL SYSTEMS

Importance of incorporating a functional vascular system into tumor models for drug screening

Although tumors start as a small group of cells through a series of acquired mutations and epigenetic changes, the final tumor is a complex tissue composed of numerous heterogeneous tumor cells and tumor-related cell groups.[95] Compared with regular 2D monolayer models, the 3D homotypic tumor spheroids can indeed restore some characteristics of solid tumors, such as their spatial constructure, physiological response, and part of gene expression.[96,97] However, they cannot truthfully represent the tumor heterogeneity and the intricate the interaction between the tumor and the local TME,[12,98–100] which are all sources of chemotherapy resistance.

In addition to its own complex cell composition, the *in vivo* tumor can also recruit neighboring normal tissue cells and transform them into parts of itself, such as cancer-associated fibroblasts[101] and tumor-associated endothelial cells.[102] Furthermore, the *in vivo* tumor can even directly incorporate an existing blood vessel to realize its own vascularization, seizing oxygen and nutrients needed for growth and eliminate waste of metabolism. The tumor vasculature can not only deliver nutrients inward but also help convey circulating tumor cells (CTCs) outward for cancer metastasis,[103,104] which accounts for 90% of cancer death.[105] As for cancer treatment, both chemotherapy and immunotherapy rely on the vasculature to transport medicine cargoes to tumors. Unlike the situation in normal tissues, the vasculature distribution inside of the tumor is random and chaotic, which makes it difficult to deliver drugs to the whole tumor and reach effective concentration.[106] Moreover, the tumor vasculature may flush away the drug cargoes before they can diffuse into the surrounding tumor tissue, which greatly weakens the medication effect. None of these above-mentioned phenomena are reflected in homotypic tumor models. Therefore, integrating proper vasculature network into the *in vitro*

tumor model should facilitate the following preclinical pharmaceutical investigation. In this pursuit, the focus of microfluidic tumor chip research has gradually transitioned from high-throughput homotypic tumor spheroids array-on-a-chip to TME reconstruction. Researchers hope to have a deeper understanding of tumorigenesis and improve drug screening efficiency by studying the process of tumor formation *in vitro*.[107]

Well-established tumor–vessel microfluidic models

For constructing more realistic *in vitro* tumor models, researchers started with co-culture/tri-culture fibroblasts, endothelial cells together with tumor cells to fabricate heterotypic tumor spheroids.[108–112] Although versatile cell–cell interaction is established, different types of cells were just rearranged and stratified into different layers rather than forming perfusable tumor vasculature inside.[113,114] To date, the most effective *in vitro* tumor vascularization strategy is to restructure TME and induce interaction between the tumor spheroid and the nearby existing blood vessel.[115–119] The tumor spheroids can both secrete growth factors to remotely manipulate blood vessels and physically interact with contacted blood vessels, which will be assimilated into tumor-associated vasculature.[120]

According to the scales of the vascular tissue, the microfluidic vessel–tumor models can be classified into three broad categories: capillary vessel–tumor model,[115,116,121] single-lumen vessel–tumor model,[118,122] and endothelium–tumor model.[123] In these three models, the relative sizes of tumor and blood vessel tissues are different, thus simulating the interaction between tumor and blood vessels at different cancer stages.

Microvessel network interacting with tumor spheroids is a widely reported method to generate a vascularized tumor spheroid model [Fig. 5(a)].[115,124,127–130] The developed tumor spheroids can secrete a series of growth factors, such as vascular endothelial growth factor (VEGF), to attract endothelial cells, self-assemble, and invade into the tumor spheroids. The diameter of the formed vessels is usually around 10 μm, and it is considered an *in vitro* reappearing of the tumor-activated angiogenesis process. After invasion, these capillary vessels will overspread and converge together in the core area of the spheroids, resulting in a perfusable vascularized tumor. Nashimoto *et al.* reported a "vascularized cancer-on-a-chip" work in 2020 [Fig. 5(b)].[125] In their study, they started with tri-culturing the tumor cells with fibroblasts and endothelial cells. Most of fibroblasts and endothelial cells were dispersed in the outer layer of the tumor core, and no vascular tube was found to form inside. Then, they planted the heterotypic tumor spheroids in the center of their microfluidic culture chip. As the spheroids grew, the fibroblasts interacted with the tumor cells and secreted angiogenic factors. Under the stimulation of these growth factors, dispersed endothelial cells (ECs) at two sides self-assembled into microvessels and then grew toward the tumor spheroids. After invading into the tumor spheroids, the vessels growing from both sides were naturally connected, which significantly increased the proliferative activity of tumor cells and reduced cell death in the spheroids. Furthermore, due to the transport function of vessels and additional drug resistance from stroma cells, these vascularized tumors showed significantly different responses to anti-cancer drugs compared to the homotypic tumor spheroid. Contrary to the results collected under static conditions, drug administrated under perfusion conditions did not show a dose-dependent effect of anti-cancer drugs on tumor activity. The potential reason may be the blood flow flushed away the drug before it could be taken up by tumor tissue via either active transport or passive diffusion. Also, Haase *et al.* found that the tumor spheroids can regulate vessel density and barrier function, thereby affecting drug transport [Fig. 5(c)].[119] Overall, these studies show that tumor vascularization significantly affects drug screening outcomes.

Notably, the current *in vitro* vascularized tumor models are most used for fundamental study since their throughput is much lower than homotypic "tumor chip" platforms. A limited number of vascularized tumors can be produced each time, and reproducibility of the method still needs to be improved. However, it is worth mentioning that there are already some tentative efforts on increasing the production of vascularized tumors for commercial applications [Fig. 5(d)].[126] In the future, a standard automated microfluidic chip platform is expected to be invented for vascularized tumor spheroid array generation and high-throughput parallel screening of multiple drugs.[131,132]

Another popular tumor–vessel interaction model is to co-culture tumor spheroids with a straight single-lumen blood vessel [Fig. 6(a)].[134–136] In general, the diameter of the single-lumen vessel tubes is around several hundred micrometers, which are small arteriole-scale blood vessels. Different from the EC self-assembled vessel network, this single-lumen vessel is constructed by covering ECs in a pre-formed hollow channel, which is built in the hydrogel with mold embedding methods. After the mold (usually needles) is removed, endothelial cell suspension will be loaded inside. Once all the endothelial cells attach and cover the whole inner surface of the channel, the endothelialization process will end. Then, tumor spheroids/organoids will be seeded around the completed vascular channel [Fig. 6(b)].[122] Based on the tumor types, matrix properties, and spatial distribution of tumors and blood vessels, different forms of tumor–vessel interactions can be recapitulated with such an approach. Kwak and Lee reported that tumor spheroids can induce capillary vessels sprouting from the single-lumen vascular channel [Fig. 6(c)].[133] Additionally, Ayuso *et al.* constructed a vessel incorporated tumor slicing model to study cell behavior under metabolic starvation gradients [Fig. 6(d)].[134] Significantly, a group from Johns Hopkins University found that breast tumors can directly fuse with normal vasculature into mosaic vessels.[137] The researchers cocultured breast tumor organoids with a straight vasculature (around 200 μm in diameter) in a matrix hydrogel. As the tumor grew, the blood vessels were constantly squeezed until they merged. Part of the tumor even became the blood vessel wall. The observed "vascular mosaicism" phenomenon has also been demonstrated in clinical gastric cancer, glioblastoma, melanoma, and other cancer cases.[138] Once tumor cells become part of blood vessels, the so-called "mosaic vessel" can provide a "highway" for circulating tumor cells (CTCs) and CTC clusters to be peeled off from the primary tumors and escape into the bloodstream. Compared with the other vascularized tumor models, this type of vessel–tumor model is simple to construct and is of great significance for understanding the cancer development.

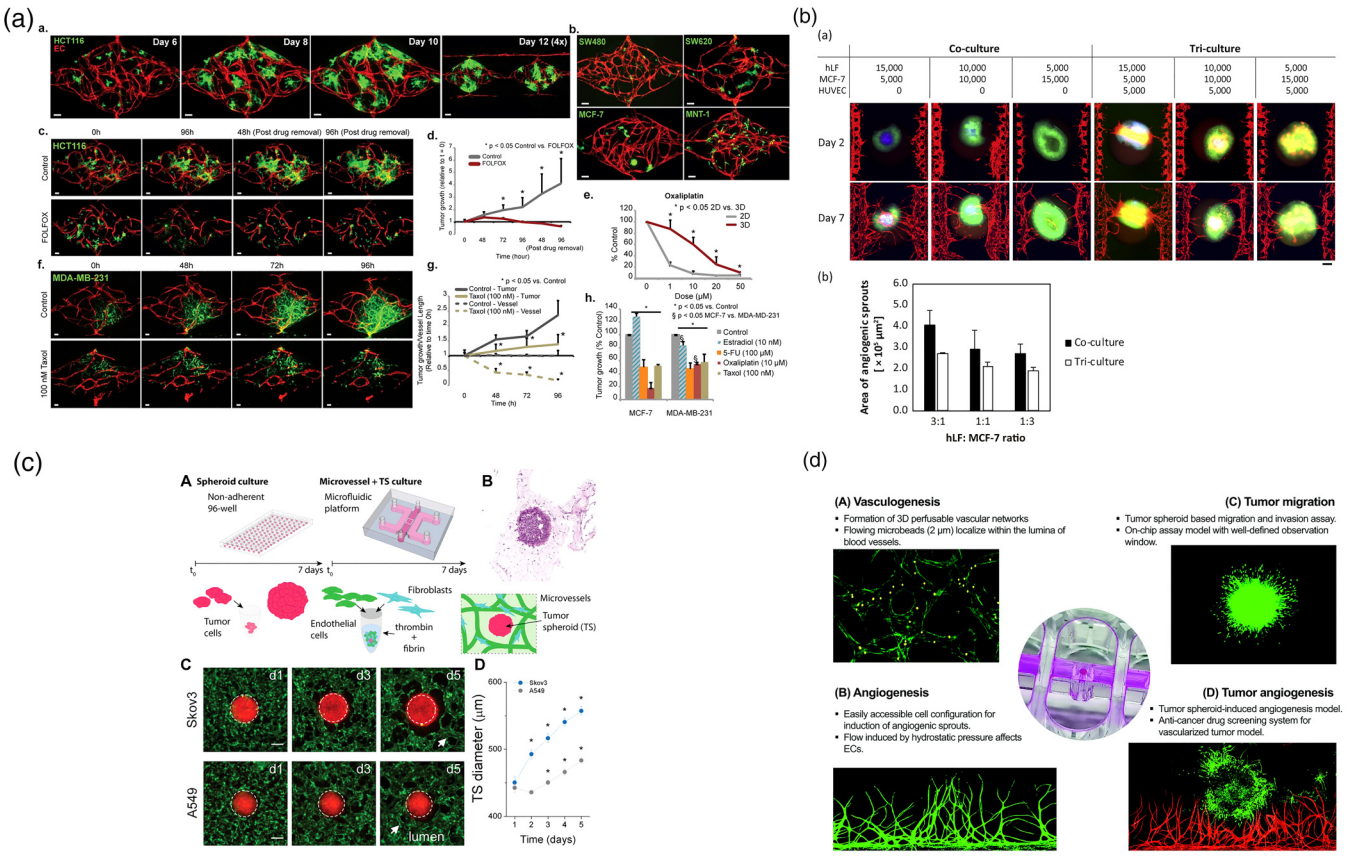

FIG. 5. Capillary vessel–tumor interaction. (a) An *in vitro* vascularized microtumor (VMT) platform to test anti-angiogenesis drugs for cancer treatment.[124] Reprinted with permission from Sobrino *et al.*, Sci. Rep. **6**, 31589 (2016). Copyright 2016 Springer Nature. (b) A tumor-on-a-chip platform that enables the evaluation of tumor activities with intraluminal flow in an engineered tumor vascular network. The fibroblasts in the tumor spheroid induced angiogenic sprouts, which constructed a perfusable vascular network in a tumor spheroid.[125] Reprinted with permission from Nashimoto *et al.*, Biomaterials **229**, 119547 (2020). Copyright 2019 Elsevier Ltd. (c) A 3D vascularized tumor-on-a-chip model is used to examine drug delivery in a relevant TME within a large bed of perfusable vasculature.[119] Reprinted with permission from Haase *et al.*, Adv. Funct. Mater. **30**, 2002444 (2020). Copyright 2020 WILEY-VCH Verlag GmbH & Co. KGaA Weinheim. (d) A standardized microfluidic culture platform for investigating tumor angiogenesis. The platform is made of polystyrene (PS) in a standardized 96-well plate and has the potential to be translated into market oriented preclinical applications.[126] Reprinted with permission from Ko *et al.*, Lab Chip **19**, 2822 (2019). Copyright 2019 The Royal Society of Chemistry.

The third type is monolayer endothelium–tumor co-culture model, which is usually exploited to model early-stage primary tumor. This model is usually composed of upper and lower two-tier structures.[131,139,140,143–148] The upper and lower layers are usually separated by a porous membrane.[142] Endothelium and epithelium are seeded on the upper and lower sides of the membrane[149] [Fig. 7(a)]. Tumor aggregates are planted above the epithelium to mimic the initial phase of cancer.[150] From an engineering point of view, it can be considered a microfluidic version of "trans-well assays."[151] At this early stage, the primary tumor is relatively small, and the pathological changes mainly occur on tumor–epithelium/endothelium interfaces. The cells cultured on surfaces of the membrane deposit their own basement membrane matrix crossing the membrane pores to help the upper and lower layers of cells to form direct interaction. The design of these devices is quite flexible. For example, hollow side chambers can be set on both sides of the tumor model. By applying circulatory ventilation in these airways, the entire device is stretched rhythmically, thereby simulating mechanical stimuli related to organs, such as blood flow and related physiological shear stress [Fig. 7(b)].[140] Choi *et al.* described a biomimetic microengineering strategy to reconstitute 3D human breast tumors located in the corresponding TME [Fig. 7(c)]. In this design, a normal mammary epithelium inlaid with the tumor clusters was reproduced on the top surface of the membrane, and a mammary fibroblast-laden stromal layer was formed on the back side. Fresh culture medium was perfused in the upper and lower channels to provide nutrition and mechanical stimulation in the bloodstream. This engineered tumor model represented the first critical step toward recapitulating pathophysiological complexity of breast cancer and may serve as a tool to systematically examine the tumor initiation, progression, and metastasis in local TME. In addition to the above-mentioned study, this membrane

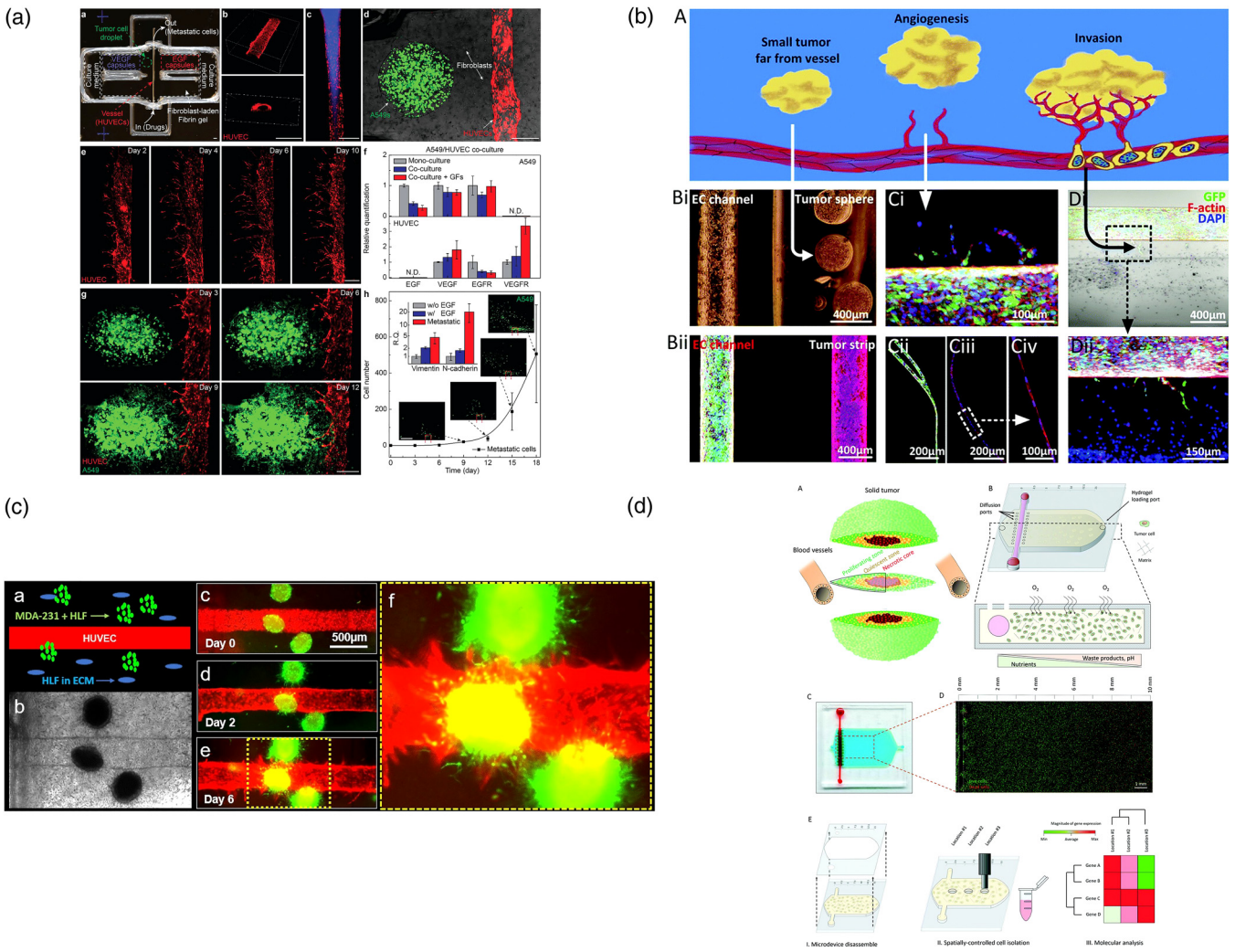

FIG. 6. Straight macro vessel–tumor interaction. (a) A bioprinted tumor–vessel co-culture model provides a platform to explore the molecular mechanisms of tumor progression and screen anti-cancer drugs.[118] Reprinted with permission from Meng *et al.*, Adv. Mater. **31**, e1806899 (2019). Copyright 2019 WILEY-VCH Verlag GmbH & Co. KGaA, Weinheim. (b) A 3D bioprinted bulk breast tumor tissue with a functional vascular network is built for physiology study and therapy evaluation.[122] Reprinted with permission from Nie *et al.*, Mater. Horiz. **7**, 82 (2020). Copyright 2020 The Royal Society of Chemistry. (c) A microfluidic model of the solid tumor–vascular interface is applied to study molecular crosstalk in tumorigenesis and cancer metastasis.[133] Reprinted with permission from Kwak and Lee, Sci. Rep. **6**, 20142 (2016). Copyright 2016 Springer Nature. (d) A microfluidic tumor slice model with a lumen on the flank of the chamber to perfuse media, mimicking the vasculature.[134] Reprinted with permission from Ayuso *et al.*, Lab Chip **19**, 3461 (2019). Copyright 2019 The Royal Society of Chemistry.

based double-layer module can be further applied in a multi-organ system or a body-on-a-chip (BOC) system. Xu *et al.* used this design to mimic the lung tissue and integrated it with three downstream "distant organs" [Fig. 7(d)].[142] In this way, cancer cell metastasis to the different organs, such as brain, bone, and liver, can be studied in an integrated system. Although these three types of microfluidic tumor/vascular models are different in spatial structure and cell composition, they simulate the interaction between tumors and blood vessels at different stages of cancer, facilitating tumor research at different stages and different purposes.

MICROFLUIDIC ORGANOID-ON-A-CHIP

From the historical development of technology, a microfluidic tumor chip is a special branch of organ chip technology in the field of oncology.[13] Organoids are miniaturized *in vitro* organ models that are mainly developed from human stem cells to mimic the critical characteristics and physiological functions of *in vivo* organs with high fidelity.[8] Compared with time-consuming and elaborate animal models, organoids allow human-derived materials to be quickly cultivated for both *in vitro* developmental biology and

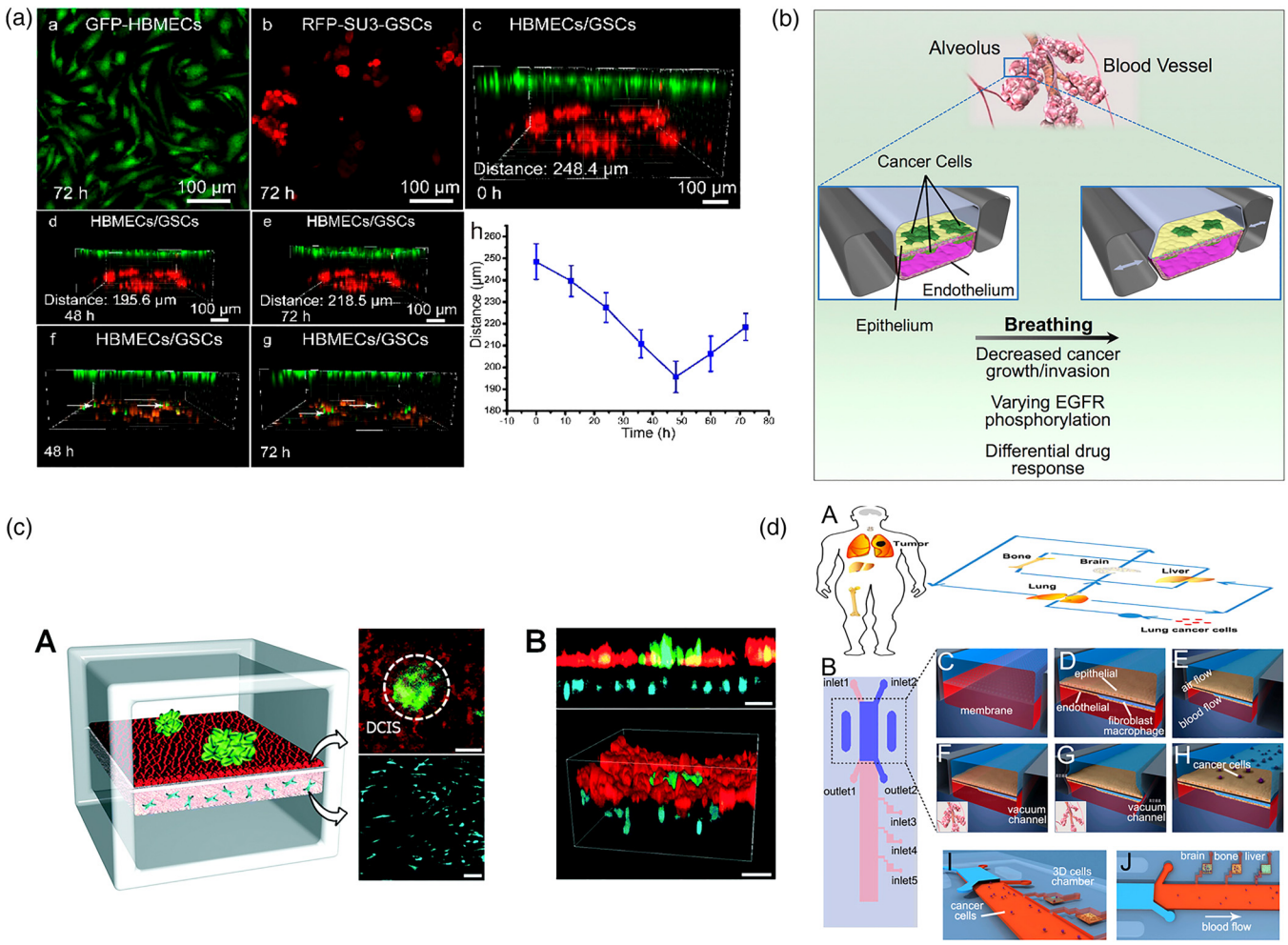

FIG. 7. Endothelium monolayer–tumor interaction. (a) A biomimetic glioma perivascular niche model on-a-chip. Glioma cancer cells and endothelial cells are planted on the upper and lower sides of a PC membrane, respectively.[139] Reprinted with permission from Lin *et al.*, Anal. Chem. **90**, 10326 (2018). Copyright 2018 American Chemical Society. (b) A microfluidic human orthotopic lung cancer-on-a-chip model. The endothelium monolayer covers the four walls of the lower channel to mimic the vessel tube. Epithelium and cancer cell aggregates are located on the top surface of the membrane.[140] Reprinted with permission from Hassell *et al.*, Cell Rep. **21**, 508 (2017). Copyright 2017 Elsevier B.V. (c) A basement membrane based microfluidic model to mimic early-stage cancerous tissue. The breast cancer spheroids are planted on the top of epithelium tissue monolayer.[141] Reprinted with permission from Choi *et al.*, Lab Chip **15**, 3350 (2015). Copyright 2015 The Royal Society of Chemistry. (d) A bilayer device to study the cancer metastasis. Cancer cells flow through the channel within the artificial blood and get trapped on the epithelium monolayer.[142] Reprinted with permission from Xu *et al.*, ACS Appl. Mater. Interfaces **8**, 25840 (2016). Copyright 2016 American Chemical Society.

pathology research.[156] In order to produce organoids in a more uniform and high-throughput way, the cultivation process gradually shifted from "in-dish" to "on-a-chip," which is the so-called "organoid-on-a-chip."[157] Here, the microfluidic chips can help strictly regulate the local microenvironment, thereby improving the reproducibility while reducing individual difference, such as morphology and gene expression. Nowadays, organoid-on-a-chip technology has attracted widespread attention. Various organ models have been reported, including, but not limited to, brain organoids[152,158,159] [Fig. 8(a)], islet organoids[153,160,161] [Fig. 8(b)], liver organoids[154,162,163] [Fig. 8(c)], and so on. In particular, if the organoids are derivative of patients' biopsy or surgically removed diseased tissue, rather than stem cells, they will be referred to as patient-derived organoids.[164] The patient-derived organoid can be used as disease model for individual patients, contributing to personal therapy and drug screening.[165] For example, Jung *et al.* reported a lung cancer organoid-on-a-chip model in 2019[155] [Fig. 8(d)]. Besides recapitulating primary small-cell lung cancer-specific characteristics, the patient-derived organoid was produced in a size-controllable manner, benefiting consecutive standard drug testing. In the next stage research, researchers will be confronted with some identical challenges, organ microenvironment

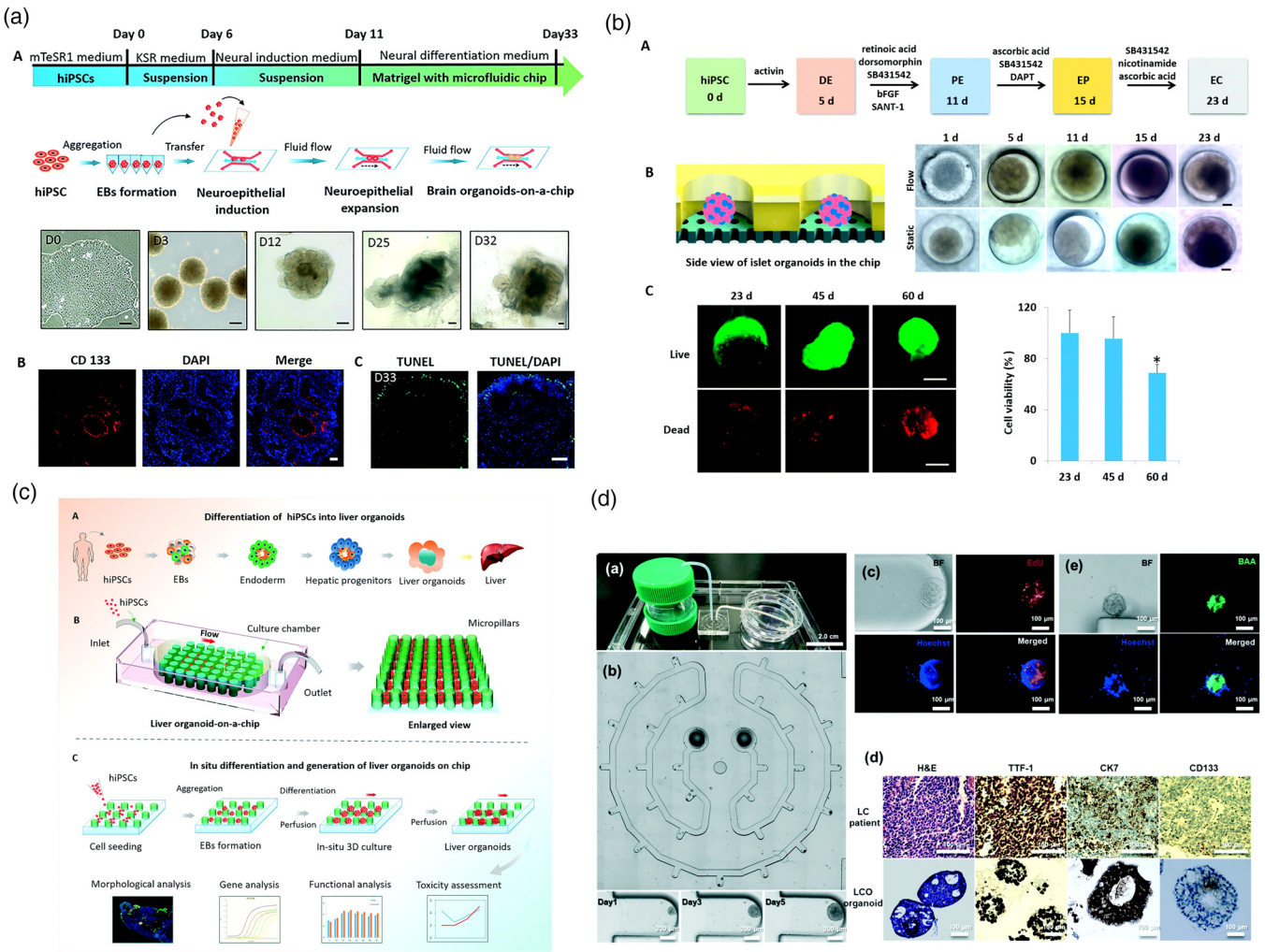

FIG. 8. Microfluidic organ/cancer organoid-on-a-chip. (a) A brain organoid-on-a-chip system is established to model neurodevelopmental disorders under nicotine exposure.[152] Reprinted with permission from Wang *et al.*, Lab Chip **18**, 851 (2018). Copyright 2018 The Royal Society of Chemistry. (b) An islet organoid-on-a-chip system enables controllable maturation of islet organoids from induced pluripotent stem cells and real-time imaging and *in situ* tracking of islet organoid growth.[153] Reprinted with permission from Tao *et al.*, Lab Chip **19**, 948 (2019). Copyright 2019 The Royal Society of Chemistry. (c) A 3D perfusable liver organoid-on-a-chip system displays improved cell viability and high-fidelity reduction of liver functions.[154] Reprinted with permission from Wang *et al.*, Lab Chip **18**, 3606 (2018). Copyright 2018 The Royal Society of Chemistry. (d) A microphysiological system reproducibly yields patient-derived small-cell lung cancer organoids in a size-controllable manner and efficiently predicts anti-cancer drug efficacy.[155] Reprinted with permission from Jung *et al.*, Lab Chip **19**, 2854 (2019). Copyright 2019 The Royal Society of Chemistry.

reconstruction and tissue vascularization. Although tumor vascularization has been demonstrated, the fragility and complexity of organ organoids make it more difficult for them to be vascularized.

PROMISING MICROSCOPIC CHARACTERIZATION AND IMAGE ANALYSIS OF TUMOR SPHEROIDS

With the progress of microfluidic technology and cancer biology, significant improvements have been made in tumor-on-a-chip model. Subsequently, the characterization methods that can collect abundant information from these tumor models have become one of the research concerns. In addition to conventional bright-field and fluorescence-assisted morphological characterization, more and more promising imaging modalities have been used to investigate microfluidic tumor models to obtain both physiological and pathological information. For example, optical coherence tomography (OCT)[144,173] has been used as a non-invasive approach to characterize the 3D structures deep inside tumor spheroids [Fig. 9(a)]. Based on the increased intrinsic optical attenuation, necrotic areas in these tumor spheroids were successfully detected, indicating a promising alternative to label-free viability testing in tumors. Moreover, multi-photon laser scanning microscopy

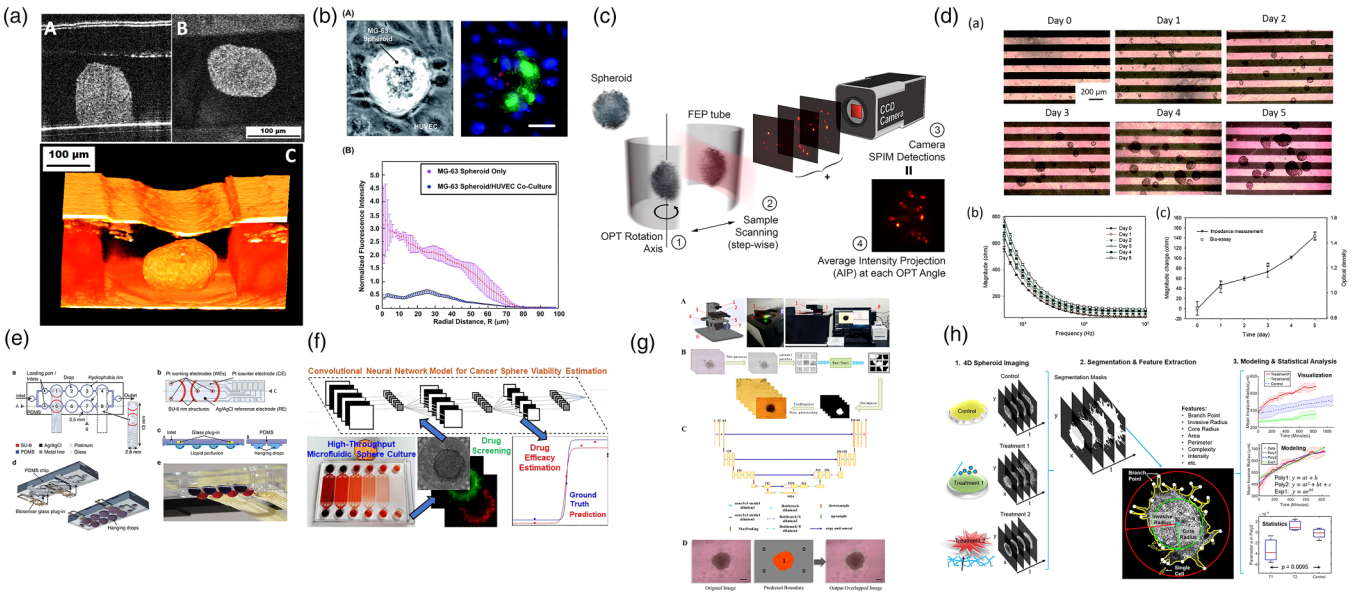

FIG. 9. Novel microtechnology-based characterization techniques integrated with tumor chips. (a) Optical coherence tomography (OCT) is employed to characterize a microfluidic bilayer vasculature/tumor co-culture model.[144] Reprinted with permission from Shi *et al.*, Biomicrofluidics **13**, 044108 (2019). Copyright 2019 AIP Publishing LLC. (b) Multi-photon laser scanning microscopy (MPLSM) is used to study oxygen tension within cocultured MG-63 spheroids and human umbilical vein endothelial cells (HUVECs) monolayers.[166] Reprinted with permission from Sarkar *et al.*, RSC Adv. **8**, 30320 (2018). Copyright 2018 The Royal Society of Chemistry. (c) Phase-retrieved tomography (PRT) is applied to radically improve mesoscopic scanning imaging of tumor spheroids.[167] Reprinted with permission from Ancora *et al.*, Sci. Rep. **7**, 11854 (2017). Copyright 2017 Springer Nature. (d) Impedance measurements are used to monitor and record the number and size of tumor spheroids in a label-free manner.[168] Reprinted with permission from Lei *et al.*, RSC Adv. **7**, 13939 (2017). Copyright 2017 The Royal Society of Chemistry. (e) Microfluidic hanging drop platform with multi-analyte biosensor for *in situ* monitoring of 3D cancer microtissue metabolism.[169] Reprinted with permission from Misun *et al.*, Microsyst. Nanoeng. **2**, 16022 (2016). Copyright 2016 Springer Nature. (f) A convolutional neural network was trained with images of LIVE/DEAD stained tumor spheroids and used to estimate spheroid viability based on its bright-field image.[170] Reprinted with permission from Zhang *et al.*, Anal. Chem. **91**, 14093 (2019). Copyright 2019 American Chemical Society. (g) A new tumor spheroid boundary detection algorithm based on convolutional neural network.[171] Reprinted with permission from Chen *et al.*, Biomaterials **272**, 120770 (2021). Copyright 2021 Elsevier Ltd. (h) Open source software for end-to-end time analysis of tumor imaging, used to automatically segment spheroid images; extract features that describe their shape, growth, and invasiveness; and perform mathematical modeling and statistical analysis on these features.[172] Reprinted with permission from Hou *et al.*, Sci. Rep. **8**, 7248 (2018). Copyright Springer Nature.

(MPLSM) [Fig. 9(b)][166] has been used to study oxygen tension variation within live tumor spheroids.[174] Phase-retrieved tomography [Fig. 9(c)][167] has been applied to improve the resolution of mesoscopic imaging on dense tumor spheroids. Along with the introduction of novel imaging approaches, various biosensors have also been integrated into microfluidic tumor chips for measuring and monitoring tumor behaviors and related microenvironments.[175] For example, Lei *et al.* incorporated interdigitated electrodes for real-time and label-free impedimetric analysis of the formation and chemosensitivity of tumor spheroids [Fig. 9(d)]. Misun *et al.* presented enzyme-based multi-analyte biosensors to enable continuous monitoring of lactate and glucose levels in cancer tissues [Fig. 9(e)]. These novel characterization technologies not only provide new perspectives for understanding tumors but also bring much unprecedented information that inspires future innovative therapies.

In addition to exploring characterization methods, how to analyze collected data in more detail has also received widespread attention. In recent years, the use of machine learning-based image processing technology on drug efficacy evaluation has become one of the research hotspots in the field of microfluidic tumor chips.[176–178] For example, Zhang *et al.* invented a microfluidic tumor-on-a-chip model, in which more than 1900 tumor spheroids were constructed for drug testing simultaneously [Fig. 9(f)].[170] The LIVE/DEAD viability staining images of the tumor spheroids were automatically collected to train a convolutional neural network (CNN), which could be used to estimate tumor spheroid viability based on its bright-field image later. Here, the microfluidic tumor chip facilitates the tumor model construction and large reliable data acquisition, and the advanced algorithms collect and process data intelligently to draw valid conclusions. It is a classic case of combining artificial intelligence (AI) and microfluidics for anti-cancer drug screening. Moreover, artificial intelligence also has unique advantages in analyzing bright-field photos of tumor spheroids. In addition to immunofluorescence staining, measuring tumor size and morphological changes is one of the most used tumor research methods. However, manual tumor imaging and hand-sketched tumor spheroid boundaries are time-consuming and subjective, and slight morphological changes are easy to be ignored. There is an urgent need for an accurate, reliable, automated, and high-throughput 3D tumor imaging analysis system. Chen *et al.* developed an automated spheroid monitoring and

AI-based recognition technique ("SMART") for analyzing tumor spheroid behavior [Fig. 9(g)].[171] Auto-recognition, auto-focusing, and an improved CNN algorithm are integrated together on this platform for automated detection of tumor spheroid boundaries. How to transform abstract morphological information into precise quantitative data has always been an unmet need of cancer researchers in the development of anti-cancer drugs. Ultimately, machine learning-based image processing is expected to help bridge the gap between physiological feature extraction and mathematical data analysis [Fig. 9(h)]. Such systems can make accurate and automatic quantitative assessments of the physiology and pathology of tumors and are of great significance for advancing emerging cell-based anti-cancer medicine.

PERSPECTIVES AND CONCLUSION

For further development, microfluidic tumor chip technology is expected to help develop cutting-edge cancer immunotherapies and achieve commercially available high-throughput preclinical drug screening. So far, only a handful of cancer immunotherapies have been approved on market, and most of them can only work on blood cancer. There are many difficulties in cell therapy for solid tumors, such as the complex heterogeneity of solid tumors, the difficulty in maintaining the viability of immune cells for a long time, and the tumor microenvironment that can inhibit immunity.[179] Recently, the immune system has been imported in some tumor-on-a-chip models for oncology immunotherapy study.[180–183] Researchers hope to figure out how to induce immune cells to break through the peripheral extracellular matrix and TME to destroy solid tumors,[184] whereas most of these immune system-tumor-on-a-chip models are still in the basic exploratory stage and the research focus remains on the direct interaction between T cells and tumors. The immunosuppressive TME and other pivotal elements, such as functional blood and lymphatic vessels, need to be incorporated into the model. Based on previous experience in building *in vitro* models for drug screening, microfluidic tumor chips can be a reliable platform to accelerate an immuno-oncology study. As for the translation of "tumor-on-a-chip" to market, the commercialization has just been unfolding. Many start-up companies and their products have sprung up, while it may take some time before pharmaceutical industries actually accept these products for preliminary drug testing.[185]

Overall, the microfluidic tumor chip is a revolutionary technology for anti-cancer drug development. Benefiting from this interdisciplinary platform, different research topics can be integrated together, such as biomechanics, immunology, and molecular biology, allowing researchers to understand cancer from new perspectives. In the foreseeable future, microfluidic tumor chip technology is promising to upgrade preclinical tumor models and shorten the translational gap between early drug discovery and clinical trials in drug developments.

ACKNOWLEDGMENTS

This work was supported by the National Institute of Health (Grant No. R01HL131750), the National Science Foundation (Grant No. CBET 2039310), and the Pennsylvania Department of Health Commonwealth Universal Research Enhancement Program (CURE).

AUTHOR DECLARATIONS

Conflicts of Interest

The authors have no conflicts to disclose.

DATA AVAILABILITY

Data sharing is not applicable to this article as no new data were created or analyzed in this study.

REFERENCES

[1]R. L. Siegel, K. D. Miller, H. E. Fuchs, and A. Jemal, CA Cancer J. Clin. **71**, 7 (2021).
[2]K. A. Conklin, Integr. Cancer Ther. **3**, 294 (2004).
[3]L. Falzone, S. Salomone, and M. Libra, Front. Pharmacol. **9**, 1300 (2018).
[4]V. Prasad and S. Mailankody, JAMA Intern. Med. **177**, 1569 (2017).
[5]T. Tammela and J. Sage, Annu. Rev. Cancer Biol. **4**, 99 (2020).
[6]K. V. Kitaeva, C. S. Rutland, A. A. Rizvanov, and V. V. Solovyeva, Front. Bioeng. Biotechnol. **8**, 322 (2020).
[7]M. Kapałczyńska, T. Kolenda, W. Przybyła, M. Zajączkowska, A. Teresiak, V. Filas, M. Ibbs, R. Bliźniak, Ł Łuczewski, and K. Lamperska, Arch. Med. Sci. **14**(4), 910–919 (2016).
[8]A. Skardal, T. Shupe, and A. Atala, Drug Discov. Today **21**, 1399 (2016).
[9]I. R. Powley, M. Patel, G. Miles, H. Pringle, L. Howells, A. Thomas, C. Kettleborough, J. Bryans, T. Hammonds, M. MacFarlane, and C. Pritchard, Br. J. Cancer **122**, 735 (2020).
[10]S. A. Langhans, Front. Pharmacol. **9**, 6 (2018).
[11]D. Hanahan and R. A. Weinberg, Cell **144**, 646 (2011).
[12]T. L. Whiteside, Oncogene **27**, 5904 (2008).
[13]A. Sontheimer-Phelps, B. A. Hassell, and D. E. Ingber, Nat. Rev. Cancer **19**, 65 (2019).
[14]M. E. Katt, A. L. Placone, A. D. Wong, Z. S. Xu, and P. C. Searson, Front. Bioeng. Biotechnol. **4**, 12 (2016).
[15]S. Nath and G. R. Devi, Pharmacol. Ther. **163**, 94 (2016).
[16]A. S. Nunes, A. S. Barros, E. C. Costa, A. F. Moreira, and I. J. Correia, Biotechnol. Bioeng. **116**, 206 (2019).
[17]C. Shao, J. Chi, H. Zhang, Q. Fan, Y. Zhao, and F. Ye, Adv. Mater. Technol. **5**, 2000183 (2020).
[18]P. Cui and S. Wang, J. Pharm. Anal. **9**, 238 (2019).
[19]H. J. Oh, J. Kim, H. Kim, N. Choi, and S. Chung, Adv. Healthcare Mater. **10**, 2002122 (2021).
[20]M. Shang, R. H. Soon, C. T. Lim, B. L. Khoo, and J. Han, Lab Chip **19**, 369 (2019).
[21]K. Jakab, C. Norotte, F. Marga, K. Murphy, G. Vunjak-Novakovic, and G. Forgacs, Biofabrication **2**, 022001 (2010).
[22]W. Mueller-Klieser, J. Cancer Res. Clin. Oncol. **113**, 101 (1987).
[23]V. E. Santo, M. F. Estrada, S. P. Rebelo, S. Abreu, I. Silva, C. Pinto, S. C. Veloso, A. T. Serra, E. Boghaert, P. M. Alves, and C. Brito, J. Biotechnol. **221**, 118 (2016).
[24]E. O. Mosaad, K. F. Chambers, K. Futrega, J. A. Clements, and M. R. Doran, Sci. Rep. **8**, 253 (2018).
[25]R. K. Vadivelu, C. H. Ooi, R.-Q. Yao, J. Tello Velasquez, E. Pastrana, J. Diaz-Nido, F. Lim, J. A. K. Ekberg, N.-T. Nguyen, and J. A. St John, Sci. Rep. **5**, 15083 (2015).
[26]W. Lim, H.-H. Hoang, D. You, J. Han, J. E. Lee, S. Kim, and S. Park, Analyst **143**, 5841 (2018).
[27]D. M. Kingsley, C. L. Roberge, A. Rudkouskaya, D. E. Faulkner, M. Barroso, X. Intes, and D. T. Corr, Acta Biomater. **95**, 357 (2019).
[28]S. M. Park, S. J. Lee, J. Lim, B. C. Kim, S. J. Han, and D. S. Kim, ACS Appl. Mater. Interfaces **10**, 37878 (2018).

[29]G. Fang, H. Lu, A. Law, D. Gallego-Ortega, D. Jin, and G. Lin, Lab Chip **19**, 4093 (2019).
[30]J. M. Lee, D. Y. Park, L. Yang, E.-J. Kim, C. D. Ahrberg, K.-B. Lee, and B. G. Chung, Sci. Rep. **8**, 17145 (2018).
[31]S.-P. Zhao, Y. Ma, Q. Lou, H. Zhu, B. Yang, and Q. Fang, Anal. Chem. **89**, 10153 (2017).
[32]R. Foty, J. Vis. Exp. e2720 (2011).
[33]A. Ganguli, A. Mostafa, C. Saavedra, Y. Kim, P. Le, V. Faramarzi, R. W. Feathers, J. Berger, K. P. Ramos-Cruz, O. Adeniba, G. J. P. Diaz, J. Drnevich, C. L. Wright, A. G. Hernandez, W. Lin, A. M. Smith, F. Kosari, G. Vasmatzis, P. Z. Anastasiadis, and R. Bashir, Sci. Adv. (**17**), eabc1323 (2021).
[34]Y.-C. Tung, A. Y. Hsiao, S. G. Allen, Y.-S. Torisawa, M. Ho, and S. Takayama, Analyst **136**, 473 (2011).
[35]A. A. Popova, T. Tronser, K. Demir, P. Haitz, K. Kuodyte, V. Starkuviene, P. Wajda, and P. A. Levkin, Small **15**, 1901299 (2019).
[36]I. J. Michael, S. Kumar, J. M. Oh, D. Kim, J. Kim, and Y.-K. Cho, ACS Appl. Mater. Interfaces **10**, 33839 (2018).
[37]L. Zhao, J. Xiu, Y. Liu, T. Zhang, W. Pan, X. Zheng, and X. Zhang, Sci. Rep. **9**, 19717 (2019).
[38]J. M. Munson and A. C. Shieh, Cancer Manage. Res. **6**, 317 (2014).
[39]R. Bashir, Adv. Drug Delivery Rev. **56**, 1565 (2004).
[40]X. Liu, J. Fang, S. Huang, X. Wu, X. Xie, J. Wang, F. Liu, M. Zhang, Z. Peng, and N. Hu, Microsyst. Nanoeng. **7**, 50 (2021).
[41]G. Luka, A. Ahmadi, H. Najjaran, E. Alocilja, M. DeRosa, K. Wolthers, A. Malki, H. Aziz, A. Althani, and M. Hoorfar, Sensors **15**, 30011 (2015).
[42]J. Zhuang, J. Zhang, M. Wu, and Y. Zhang, Adv. Sci. **6**, 1901462 (2019).
[43]Y. Chen, D. Gao, Y. Wang, S. Lin, and Y. Jiang, Anal. Chim. Acta **1036**, 97 (2018).
[44]W. Liu, J.-C. Wang, and J. Wang, Lab Chip **15**, 1195 (2015).
[45]Y. Fan, D. T. Nguyen, Y. Akay, F. Xu, and M. Akay, Sci. Rep. **6**, 25062 (2016).
[46]K. Lee, C. Kim, J. Young Yang, H. Lee, B. Ahn, L. Xu, J. Yoon Kang, and K. W. Oh, Biomicrofluidics **6**, 014114 (2012).
[47]M. Marimuthu, N. Rousset, A. St-Georges-Robillard, M. A. Lateef, M. Ferland, A.-M. Mes-Masson, and T. Gervais, Lab Chip **18**, 304 (2018).
[48]Y. Xu, F. Xie, T. Qiu, L. Xie, W. Xing, and J. Cheng, Biomicrofluidics **6**, 016504 (2012).
[49]T. Anada, T. Masuda, Y. Honda, J. Fukuda, F. Arai, T. Fukuda, and O. Suzuki, Sens. Actuators B **147**, 376 (2010).
[50]W. Liu, M. Sun, B. Lu, M. Yan, K. Han, and J. Wang, Sens. Actuators B **292**, 111 (2019).
[51]H. Li, T. Garner, F. Diaz, and P. K. Wong, Small **15**, 1901910 (2019).
[52]T. Mulholland, M. McAllister, S. Patek, D. Flint, M. Underwood, A. Sim, J. Edwards, and M. Zagnoni, Sci. Rep. **8**, 14672 (2018).
[53]B. Patra, C.-C. Peng, W.-H. Liao, C.-H. Lee, and Y.-C. Tung, Sci. Rep. **6**, 21061 (2016).
[54]L. Zhao, M. Shi, Y. Liu, X. Zheng, J. Xiu, Y. Liu, L. Tian, H. Wang, M. Zhang, and X. Zhang, Anal. Chem. **91**, 4307 (2019).
[55]L. Zhao, S. Mok, and C. Moraes, Biofabrication **11**, 045013 (2019).
[56]K. Kwapiszewska, A. Michalczuk, M. Rybka, R. Kwapiszewski, and Z. Brzózka, Lab Chip **14**, 2096 (2014).
[57]K. Ziółkowska, A. Stelmachowska, R. Kwapiszewski, M. Chudy, A. Dybko, and Z. Brzózka, Biosens. Bioelectron. **40**, 68 (2013).
[58]L. Zhao, Y. Liu, Y. Liu, M. Zhang, and X. Zhang, Anal. Chem. **92**, 7638 (2020).
[59]N. Dadgar, A. M. Gonzalez-Suarez, P. Fattahi, X. Hou, J. S. Weroha, A. Gaspar-Maia, G. Stybayeva, and A. Revzin, Microsyst. Nanoeng. **6**, 93 (2020).
[60]M. I. Khot, M. A. Levenstein, G. N. de Boer, G. Armstrong, T. Maisey, H. S. Svavarsdottir, H. Andrew, S. L. Perry, N. Kapur, and D. G. Jayne, Sci. Rep. **10**, 15915 (2020).
[61]L. Pang, J. Ding, Y. Ge, J. Fan, and S.-K. Fan, Anal. Chem. **91**, 8318 (2019).
[62]L. Yu, M. C. W. Chen, and K. C. Cheung, Lab Chip **10**, 2424 (2010).
[63]P. Sabhachandani, V. Motwani, N. Cohen, S. Sarkar, V. Torchilin, and T. Konry, Lab Chip **16**, 497 (2016).
[64]W. Liu, J. Xu, T. Li, L. Zhao, C. Ma, S. Shen, and J. Wang, Anal. Chem. **87**, 9752 (2015).
[65]C.-Y. Fu, S.-Y. Tseng, S.-M. Yang, L. Hsu, C.-H. Liu, and H.-Y. Chang, Biofabrication **6**, 015009 (2014).
[66]W. Liu, D. Liu, R. Hu, Z. Huang, M. Sun, and K. Han, Analyst **145**, 6447 (2020).
[67]Y. Chen, D. Gao, H. Liu, S. Lin, and Y. Jiang, Anal. Chim. Acta **898**, 85 (2015).
[68]Y. L. Huang, Y. Ma, C. Wu, C. Shiau, J. E. Segall, and M. Wu, Sci. Rep. **10**, 9648 (2020).
[69]B. Kwak, Y. Lee, J. Lee, S. Lee, and J. Lim, J. Controlled Release **275**, 201 (2018).
[70]J. M. Lee, J. W. Choi, C. D. Ahrberg, H. W. Choi, J. H. Ha, S. G. Mun, S. J. Mo, and B. G. Chung, Microsyst. Nanoeng. **6**, 52 (2020).
[71]H. Wang, P. Agarwal, B. Jiang, S. Stewart, X. Liu, Y. Liang, B. Hancioglu, A. Webb, J. P. Fisher, Z. Liu, X. Lu, K. H. R. Tkaczuk, and X. He, Adv. Sci. **7**, 2000259 (2020).
[72]P. Sabhachandani, S. Sarkar, S. Mckenney, D. Ravi, A. M. Evens, and T. Konry, J. Controlled Release **295**, 21 (2019).
[73]S. Yoon, J. A. Kim, S. H. Lee, M. Kim, and T. H. Park, Lab Chip **13**, 1522 (2013).
[74]P. Agarwal, H. Wang, M. Sun, J. Xu, S. Zhao, Z. Liu, K. J. Gooch, Y. Zhao, X. Lu, and X. He, ACS Nano **11**, 6691 (2017).
[75]X. Cui, Y. Liu, Y. Hartanto, J. Bi, S. Dai, and H. Zhang, Colloids Interface Sci. Commun. **14**, 4 (2016).
[76]Y. Wang and J. Wang, Analyst **139**, 2449 (2014).
[77]A. Huebner, S. Sharma, M. Srisa-Art, F. Hollfelder, J. B. Edel, and A. J. Demello, Lab Chip **8**, 1244 (2008).
[78]Z. Wu, Z. Gong, Z. Ao, J. Xu, H. Cai, M. Muhsen, S. Heaps, M. Bondesson, S. Guo, and F. Guo, ACS Appl. Bio Mater. **3**, 6273–6283 (2020).
[79]Q. Sun, S. H. Tan, Q. Chen, R. Ran, Y. Hui, D. Chen, and C.-X. Zhao, ACS Biomater. Sci. Eng. **4**, 4425 (2018).
[80]S. Sart, R. F.-X. Tomasi, G. Amselem, and C. N. Baroud, Nat. Commun. **8**(1), 469 (2017).
[81]S. Li, K. Yang, X. Chen, X. Zhu, H. Zhou, P. Li, Y. Chen, Y. Jiang, T. Li, X. Qin, H. Yang, C. Wu, B. Ji, F. You, and Y. Liu, Biofabrication **13**, 045013 (2021).
[82]B. Samara, M. Deliorman, P. Sukumar, and M. A. Qasaimeh, Lab Chip **21**, 844-854 (2021).
[83]W. Shi, J. Kwon, Y. Huang, J. Tan, C. G. Uhl, R. He, C. Zhou, and Y. Liu, Sci. Rep. **8**(1), 6837 (2018).
[84]H. Tseng, J. A. Gage, T. Shen, W. L. Haisler, S. K. Neeley, S. Shiao, J. Chen, P. K. Desai, A. Liao, C. Hebel, R. M. Raphael, J. L. Becker, and G. R. Souza, Sci. Rep. **5**, 13987 (2015).
[85]V. H. B. Ho, K. H. Müller, A. Barcza, R. Chen, and N. K. H. Slater, Biomaterials **31**, 3095 (2010).
[86]A. Tocchio, N. G. Durmus, K. Sridhar, V. Mani, B. Coskun, R. El Assal, and U. Demirci, Adv. Mater. **30**, 1705034 (2018).
[87]J. E. Perez, I. Nagle, and C. Wilhelm, Biofabrication **13**, 015018 (2020).
[88]G. R. Souza, J. R. Molina, R. M. Raphael, M. G. Ozawa, D. J. Stark, C. S. Levin, L. F. Bronk, J. S. Ananta, J. Mandelin, M.-M. Georgescu, J. A. Bankson, J. G. Gelovani, T. C. Killian, W. Arap, and R. Pasqualini, Nat. Nanotechnol. **5**, 291 (2010).
[89]X. Hu, S. Zhao, Z. Luo, Y. Zuo, F. Wang, J. Zhu, L. Chen, D. Yang, Y. Zheng, Y. Zheng, Y. Cheng, F. Zhou, and Y. Yang, Lab Chip **20**, 2228 (2020).
[90]B. Chen, Y. Wu, Z. Ao, H. Cai, A. Nunez, Y. Liu, J. Foley, K. Nephew, X. Lu, and F. Guo, Lab Chip **19**, 1755 (2019).
[91]K. Olofsson, V. Carannante, M. Ohlin, T. Frisk, K. Kushiro, M. Takai, A. Lundqvist, B. Önfelt, and M. Wiklund, Lab Chip **18**, 2466-2476 (2018).
[92]K. Chen, M. Wu, F. Guo, P. Li, C. Y. Chan, Z. Mao, S. Li, L. Ren, R. Zhang, and T. J. Huang, Lab Chip **16**, 2636 (2016).
[93]W. Lim and S. Park, Molecules **23**, 3355 (2018).
[94]T. Petreus, E. Cadogan, G. Hughes, A. Smith, V. Pilla Reddy, A. Lau, M. J. O'Connor, S. Critchlow, M. Ashford, and L. Oplustil O'Connor, Commun. Biol. **4**, 1001 (2021).
[95]C. E. Meacham and S. J. Morrison, Nature **501**, 328 (2013).
[96]H. Kim, Y. Phung, and M. Ho, PLoS ONE **7**, e39556 (2012).

[97]A. C. Luca, S. Mersch, R. Deenen, S. Schmidt, I. Messner, K.-L. Schäfer, S. E. Baldus, W. Huckenbeck, R. P. Piekorz, W. T. Knoefel, A. Krieg, and N. H. Stoecklein, PLoS ONE **8**, e59689 (2013).
[98]H.-G. Yi, Y. H. Jeong, Y. Kim, Y.-J. Choi, H. E. Moon, S. H. Park, K. S. Kang, M. Bae, J. Jang, H. Youn, S. H. Paek, and D.-W. Cho, Nat. Biomed. Eng. **3**, 509 (2019).
[99]K. Chen, E. Jiang, X. Wei, Y. Xia, Z. Wu, Z. Gong, Z. Shang, and S. Guo, Lab Chip **21**, 1604-1612 (2021).
[100]M. Tang, S. K. Tiwari, K. Agrawal, M. Tan, J. Dang, T. Tam, J. Tian, X. Wan, J. Schimelman, S. You, Q. Xia, T. M. Rana, and S. Chen, Small **17**, 2006050 (2021).
[101]F. Xing, Front. Biosci. **15**, 166 (2010).
[102]K. Hida, Y. Hida, D. N. Amin, A. F. Flint, D. Panigrahy, C. C. Morton, and M. Klagsbrun, Cancer Res. **64**, 8249 (2004).
[103]J. P. Sleeman and W. Thiele, Int. J. Cancer **125**, 2747 (2009).
[104]S. Wang, Y. Zhou, X. Qin, S. Nair, X. Huang, and Y. Liu, Sci. Rep. **10**, 12226 (2020).
[105]T. N. Seyfried and L. C. Huysentruyt, Crit. Rev. Oncog. **18**, 43 (2013).
[106]D. W. Siemann, Cancer Treat. Rev. **37**, 63 (2011).
[107]H. N. Kim, N. L. Habbit, C. Su, N. Choi, E. H. Ahn, E. A. Lipke, and D. Kim, Adv. Funct. Mater. **29**, 1807553 (2019).
[108]S. Herter, L. Morra, R. Schlenker, J. Sulcova, L. Fahrni, I. Waldhauer, S. Lehmann, T. Reisländer, I. Agarkova, J. M. Kelm, C. Klein, P. Umana, and M. Bacac, Cancer Immunol. Immunother. **66**, 129 (2017).
[109]J. Antunes, V. M. Gaspar, L. Ferreira, M. Monteiro, R. Henrique, C. Jerónimo, and J. F. Mano, Acta Biomater. **94**, 392 (2019).
[110]I. Yakavets, S. Jenard, A. Francois, Y. Maklygina, V. Loschenov, H.-P. Lassalle, G. Dolivet, and L. Bezdetnaya, J. Clin. Med. **8**, 1686 (2019).
[111]S. P. Carey, A. Starchenko, A. L. McGregor, and C. A. Reinhart-King, Clin. Exp. Metastasis **30**, 615 (2013).
[112]L. De Moor, I. Merovci, S. Baetens, J. Verstraeten, P. Kowalska, D. V. Krysko, W. H. De Vos, and H. Declercq, Biofabrication **10**, 035009 (2018).
[113]G. Lazzari, V. Nicolas, M. Matsusaki, M. Akashi, P. Couvreur, and S. Mura, Acta Biomater. **78**, 296 (2018).
[114]Z. Wu, B. Chen, Y. Wu, Y. Xia, H. Chen, Z. Gong, H. Hu, Z. Ding, and S. Guo, Lab Chip **21**, 3498-3508 (2021).
[115]S. M. Ehsan, K. M. Welch-Reardon, M. L. Waterman, C. C. W. Hughes, and S. C. George, Integr. Biol. **6**, 603 (2014).
[116]S. J. Hachey, S. Movsesyan, Q. H. Nguyen, G. Burton-Sojo, A. Tankazyan, J. Wu, T. Hoang, D. Zhao, S. Wang, M. M. Hatch, E. Celaya, S. Gomez, G. T. Chen, R. T. Davis, K. Nee, N. Pervolarakis, D. A. Lawson, K. Kessenbrock, A. P. Lee, J. Lowengrub, M. L. Waterman, and C. C. W. Hughes, Lab Chip **21**, 1333-1351 (2021).
[117]M. S. Singh, M. Goldsmith, K. Thakur, S. Chatterjee, D. Landesman-Milo, T. Levy, L. A. Kunz-Schughart, Y. Barenholz, and D. Peer, Nanoscale **12**, 1894 (2020).
[118]F. Meng, C. M. Meyer, D. Joung, D. A. Vallera, M. C. McAlpine, and A. Panoskaltsis-Mortari, Adv. Mater. **31**, 1806899 (2019).
[119]K. Haase, G. S. Offeddu, M. R. Gillrie, and R. D. Kamm, Adv. Funct. Mater. **30**, 2002444 (2020).
[120]J. M. Pluda, Semin. Oncol. **24**, 203 (1997).
[121]E. Sano, C. Mori, Y. Nashimoto, R. Yokokawa, H. Kotera, and Y.-S. Torisawa, Biomicrofluidics **12**, 042204 (2018).
[122]J. Nie, Q. Gao, C. Xie, S. Lv, J. Qiu, Y. Liu, M. Guo, R. Guo, J. Fu, and Y. He, Mater. Horiz. **7**, 82 (2020).
[123]H.-F. Wang, R. Ran, Y. Liu, Y. Hui, B. Zeng, D. Chen, D. A. Weitz, and C.-X. Zhao, ACS Nano **12**, 11600 (2018).
[124]A. Sobrino, D. T. T. Phan, R. Datta, X. Wang, S. J. Hachey, M. Romero-López, E. Gratton, A. P. Lee, S. C. George, and C. C. W. Hughes, Sci. Rep. **6**, 31589 (2016).
[125]Y. Nashimoto, R. Okada, S. Hanada, Y. Arima, K. Nishiyama, T. Miura, and R. Yokokawa, Biomaterials **229**, 119547 (2020).
[126]J. Ko, J. Ahn, S. Kim, Y. Lee, J. Lee, D. Park, and N. L. Jeon, Lab Chip **19**, 2822 (2019).
[127]J. Paek, S. E. Park, Q. Lu, K.-T. Park, M. Cho, J. M. Oh, K. W. Kwon, Y.-S. Yi, J. W. Song, H. I. Edelstein, J. Ishibashi, W. Yang, J. W. Myerson, R. Y. Kiseleva, P. Aprelev, E. D. Hood, D. Stambolian, P. Seale, V. R. Muzykantov, and D. Huh, ACS Nano **13**, 7627 (2019).
[128]S. Oh, H. Ryu, D. Tahk, J. Ko, Y. Chung, H. K. Lee, T. R. Lee, and N. L. Jeon, Lab Chip **17**, 3405 (2017).
[129]M. Dey, B. Ayan, M. Yurieva, D. Unutmaz, and I. T. Ozbolat, Adv Biol. **5**, 2100090 (2021).
[130]C. Li, S. Li, K. Du, P. Li, B. Qiu, and W. Ding, ACS Appl. Mater. Interfaces **13**, 19768 (2021).
[131]S. W. Lee, S. Hong, B. Jung, S. Y. Jeong, J. H. Byeon, G. S. Jeong, J. Choi, and C. Hwang, Biotechnol. Bioeng. **116**, 3041 (2019).
[132]P. Järvinen, A. Bonabi, V. Jokinen, and T. Sikanen, Adv. Funct. Mater. **30**, 2000479 (2020).
[133]T. J. Kwak and E. Lee, Sci. Rep. **10**, 20142 (2020).
[134]J. M. Ayuso, M. Virumbrales-Munoz, P. H. McMinn, S. Rehman, I. Gomez, M. R. Karim, R. Trusttchel, K. B. Wisinski, D. J. Beebe, and M. C. Skala, Lab Chip **19**, 3461 (2019).
[135]S. C. Kerr, M. M. Morgan, A. A. Gillette, M. K. Livingston, K. M. Lugo-Cintron, P. F. Favreau, L. Florek, B. P. Johnson, J. M. Lang, M. C. Skala, and D. J. Beebe, Integr. Biol. **12**, 250 (2020).
[136]M. Humayun, J. M. Ayuso, R. A. Brenneke, M. Virumbrales-Muñoz, K. Lugo-Cintrón, S. Kerr, S. M. Ponik, and D. J. Beebe, Biomaterials **270**, 120640 (2021).
[137]V. L. Silvestri, E. Henriet, R. M. Linville, A. D. Wong, P. C. Searson, and A. J. Ewald, Cancer Res. **80**, 4288 (2020).
[138]Y. S. Chang, E. di Tomaso, D. M. McDonald, R. Jones, R. K. Jain, and L. L. Munn, Proc. Natl. Acad. Sci. U.S.A. **97**, 14608 (2000).
[139]C. Lin, L. Lin, S. Mao, L. Yang, L. Yi, X. Lin, J. Wang, Z.-X. Lin, and J.-M. Lin, Anal. Chem. **90**, 10326 (2018).
[140]B. A. Hassell, G. Goyal, E. Lee, A. Sontheimer-Phelps, O. Levy, C. S. Chen, and D. E. Ingber, Cell Rep. **21**, 508 (2017).
[141]Y. Choi, E. Hyun, J. Seo, C. Blundell, H. C. Kim, E. Lee, S. H. Lee, A. Moon, W. K. Moon, and D. Huh, Lab Chip **15**, 3350 (2015).
[142]Z. Xu, E. Li, Z. Guo, R. Yu, H. Hao, Y. Xu, Z. Sun, X. Li, J. Lyu, and Q. Wang, ACS Appl. Mater. Interfaces **8**, 25840 (2016).
[143]Y. Tang, F. Soroush, J. B. Sheffield, B. Wang, B. Prabhakarpandian, and M. F. Kiani, Sci. Rep. **7**, 9359 (2017).
[144]W. Shi, L. Reid, Y. Huang, C. G. Uhl, R. He, C. Zhou, and Y. Liu, Biomicrofluidics **13**, 044108 (2019).
[145]J. W. Song, S. P. Cavnar, A. C. Walker, K. E. Luker, M. Gupta, Y.-C. Tung, G. D. Luker, and S. Takayama, PLoS ONE **4**, e5756 (2009).
[146]A. Marturano-Kruik, M. M. Nava, K. Yeager, A. Chramiec, L. Hao, S. Robinson, E. Guo, M. T. Raimondi, and G. Vunjak-Novakovic, Proc. Natl. Acad. Sci. U.S.A. **115**, 1256 (2018).
[147]B. Jing, Y. Luo, B. Lin, J. Li, Z. A. Wang, and Y. Du, RSC Adv. **9**, 17137 (2019).
[148]C. G. Uhl and Y. Liu, Lab Chip **19**, 1458 (2019).
[149]A. Thomas, H. Daniel Ou-Yang, L. Lowe-Krentz, V. R. Muzykantov, and Y. Liu, Biomicrofluidics **10**, 014101 (2016).
[150]M. J. Mondrinos, Y.-S. Yi, N.-K. Wu, X. Ding, and D. Huh, Lab Chip **17**, 3146 (2017).
[151]D. Gioeli, C. J. Snow, M. B. Simmers, S. A. Hoang, R. A. Figler, J. A. Allende, D. G. Roller, J. T. Parsons, J. D. Wulfkuhle, E. F. Petricoin, T. W. Bauer, and B. R. Wamhoff, Lab Chip **19**, 1193 (2019).
[152]Y. Wang, L. Wang, Y. Zhu, and J. Qin, Lab Chip **18**, 851 (2018).
[153]T. Tao, Y. Wang, W. Chen, Z. Li, W. Su, Y. Guo, P. Deng, and J. Qin, Lab Chip **19**, 948 (2019).
[154]Y. Wang, H. Wang, P. Deng, W. Chen, Y. Guo, T. Tao, and J. Qin, Lab Chip **18**, 3606 (2018).

[155]D. J. Jung, T. H. Shin, M. Kim, C. O. Sung, S. J. Jang, and G. S. Jeong, Lab Chip **19**, 2854 (2019).
[156]M. A. Lancaster and J. A. Knoblich, Science **345**, 1247125 (2014).
[157]S. E. Park, A. Georgescu, and D. Huh, Science **364**, 960 (2019).
[158]E. Karzbrun, A. Kshirsagar, S. R. Cohen, J. H. Hanna, and O. Reiner, Nat. Phys. **14**, 515 (2018).
[159]Z. Ao, H. Cai, D. J. Havert, Z. Wu, Z. Gong, J. M. Beggs, K. Mackie, and F. Guo, Anal. Chem. **92**, 4630 (2020).
[160]S. N. Patel, M. Ishahak, D. Chaimov, A. Velraj, D. LaShoto, D. W. Hagan, P. Buchwald, E. A. Phelps, A. Agarwal, and C. L. Stabler, Sci. Adv. **7**, eaba5515 (2021).
[161]P. Sokolowska, K. Zukowski, J. Janikiewicz, E. Jastrzebska, A. Dobrzyn, and Z. Brzozka, Biosens. Bioelectron. **183**, 113215 (2021).
[162]F. Yu, R. Deng, W. Hao Tong, L. Huan, N. Chan Way, A. IslamBadhan, C. Iliescu, and H. Yu, Sci. Rep. **7**, 14528 (2017).
[163]T. Takebe, K. Sekine, M. Enomura, H. Koike, M. Kimura, T. Ogaeri, R.-R. Zhang, Y. Ueno, Y.-W. Zheng, N. Koike, S. Aoyama, Y. Adachi, and H. Taniguchi, Nature **499**, 481 (2013).
[164]E. Driehuis, K. Kretzschmar, and H. Clevers, Nat. Protoc. **15**, 3380 (2020).
[165]M. R. Carvalho, D. Barata, L. M. Teixeira, S. Giselbrecht, R. L. Reis, J. M. Oliveira, R. Truckenmüller, and P. Habibovic, Sci. Adv. **5**, 1317 (2019).
[166]S. Sarkar, C.-C. Peng, C. W. Kuo, D.-Y. Chueh, H.-M. Wu, Y.-H. Liu, P. Chen, and Y.-C. Tung, RSC Adv. **8**, 30320 (2018).
[167]D. Ancora, D. Di Battista, G. Giasafaki, S. E. Psycharakis, E. Liapis, J. Ripoll, and G. Zacharakis, Sci. Rep. **7**, 11854 (2017).
[168]K. F. Lei, B.-Y. Lin, and N.-M. Tsang, RSC Adv. **7**, 13939 (2017).
[169]P. M. Misun, J. Rothe, Y. R. F. Schmid, A. Hierlemann, and O. Frey, Microsyst. Nanoeng. **2**, 16022 (2016).
[170]Z. Zhang, L. Chen, Y. Wang, T. Zhang, Y.-C. Chen, and E. Yoon, Anal. Chem. **91**, 14093 (2019).
[171]Z. Chen, N. Ma, X. Sun, Q. Li, Y. Zeng, F. Chen, S. Sun, J. Xu, J. Zhang, H. Ye, J. Ge, Z. Zhang, X. Cui, K. Leong, Y. Chen, and Z. Gu, Biomaterials **272**, 120770 (2021).
[172]Y. Hou, J. Konen, D. J. Brat, A. I. Marcus, and L. A. D. Cooper, Sci. Rep. **8**, 7248 (2018).
[173]Y. Huang, S. Wang, Q. Guo, S. Kessel, I. Rubinoff, L. L.-Y. Chan, P. Li, Y. Liu, J. Qiu, and C. Zhou, Cancer Res. **77**, 6011 (2017).
[174]H. Wu, Y. Yang, P. O. Bagnaninchi, and J. Jia, Analyst **143**, 4189-4198 (2018).
[175]B. Patra, M. Sharma, W. Hale, and M. Utz, Sci. Rep. **11**, 53 (2021).
[176]F. Mittler, P. Obeïd, A. V. Rulina, V. Haguet, X. Gidrol, and M. Y. Balakirev, Front. Oncol. **7**, 293 (2017).
[177]L. Benning, A. Peintner, G. Finkenzeller, and L. Peintner, Sci. Rep. **10**, 11071 (2020).
[178]I. Grexa, A. Diosdi, M. Harmati, A. Kriston, N. Moshkov, K. Buzas, V. Pietiäinen, K. Koos, and P. Horvath, Sci. Rep. **11**, 14813 (2021).
[179]J. Xin Yu, V. M. Hubbard-Lucey, and J. Tang, Nat. Rev. Drug Discovery **18**, 821 (2019).
[180]S. W. L. Lee, G. Adriani, E. Ceccarello, A. Pavesi, A. T. Tan, A. Bertoletti, R. D. Kamm, and S. C. Wong, Front. Immunol. **9**, 416 (2018).
[181]X. Cui, C. Ma, V. Vasudevaraja, J. Serrano, J. Tong, Y. Peng, M. Delorenzo, G. Shen, J. Frenster, R.-T. T. Morales, W. Qian, A. Tsirigos, A. S. Chi, R. Jain, S. C. Kurz, E. P. Sulman, D. G. Placantonakis, M. Snuderl, and W. Chen, eLife **9**, e52253 (2020).
[182]A. Aung, V. Kumar, J. Theprungsirikul, S. K. Davey, and S. Varghese, Cancer Res. **80**, 263 (2020).
[183]R. W. Jenkins, A. R. Aref, P. H. Lizotte, E. Ivanova, S. Stinson, C. W. Zhou, M. Bowden, J. Deng, H. Liu, D. Miao, M. X. He, W. Walker, G. Zhang, T. Tian, C. Cheng, Z. Wei, S. Palakurthi, M. Bittinger, H. Vitzthum, J. W. Kim, A. Merlino, M. Quinn, C. Venkataramani, J. A. Kaplan, A. Portell, P. C. Gokhale, B. Phillips, A. Smart, A. Rotem, R. E. Jones, L. Keogh, M. Anguiano, L. Stapleton, Z. Jia, M. Barzily-Rokni, I. Cañadas, T. C. Thai, M. R. Hammond, R. Vlahos, E. S. Wang, H. Zhang, S. Li, G. J. Hanna, W. Huang, M. P. Hoang, A. Piris, J.-P. Eliane, A. O. Stemmer-Rachamimov, L. Cameron, M.-J. Su, P. Shah, B. Izar, M. Thakuria, N. R. LeBoeuf, G. Rabinowits, V. Gunda, S. Parangi, J. M. Cleary, B. C. Miller, S. Kitajima, R. Thummalapalli, B. Miao, T. U. Barbie, V. Sivathanu, J. Wong, W. G. Richards, R. Bueno, C. H. Yoon, J. Miret, M. Herlyn, L. A. Garraway, E. M. Van Allen, G. J. Freeman, P. T. Kirschmeier, J. H. Lorch, P. A. Ott, F. S. Hodi, K. T. Flaherty, R. D. Kamm, G. M. Boland, K.-K. Wong, D. Dornan, C. P. Paweletz, and D. A. Barbie, Cancer Discovery **8**, 196 (2018).
[184]E. Driehuis, S. Kolders, S. Spelier, K. Lõhmussaar, S. M. Willems, L. A. Devriese, R. de Bree, E. J. de Ruiter, J. Korving, H. Begthel, J. H. van Es, V. Geurts, G.-W. He, R. H. van Jaarsveld, R. Oka, M. J. Muraro, J. Vivié, M. M. J. M. Zandvliet, A. P. A. Hendrickx, N. Iakobachvili, P. Sridevi, O. Kranenburg, R. van Boxtel, G. J. P. L. Kops, D. A. Tuveson, P. J. Peters, A. van Oudenaarden, and H. Clevers, Cancer Discovery **9**, 852 (2019).
[185]C. Ma, Y. Peng, H. Li, and W. Chen, Trends Pharmacol. Sci. **42**, 119 (2021).